



ELSEVIER

Contents lists available at ScienceDirect

## Progress in Oceanography

journal homepage: [www.elsevier.com/locate/pocean](http://www.elsevier.com/locate/pocean)

## Seasonality in the cross-shelf physical structure of a temperate shelf sea and the implications for nitrate supply

Eugenio Ruiz-Castillo<sup>a,\*</sup>, Jonathan Sharples<sup>a</sup>, Jo Hopkins<sup>b</sup>, Malcolm Woodward<sup>c</sup>

<sup>a</sup> School of Environmental Sciences, University of Liverpool, L69 3GP, UK

<sup>b</sup> National Oceanography Centre, Liverpool L3 5DA, UK

<sup>c</sup> Plymouth Marine Laboratory, Plymouth PL1 3DH, UK

### ABSTRACT

We address a long-standing problem of how nutrients are transported from the shelf edge and from rivers to support regular, seasonal primary production in the interior of a wide, temperate, shelf sea. Cross-shelf sections of hydrography and nutrients, from a series of cruises between March 2014 and August 2015, along with time series of river discharge and river nutrient load are used to assess the seasonality of cross-shelf transports. Riverine nitrogen inputs are estimated to account for 30% of the nitrate available for the spring bloom on the inner shelf, and 10% in the mid- to outer-shelf. In the bottom layer in summer, high salinity, nutrient-rich waters are transported on-shelf as a result of wind-driven Ekman transport, cross-shelf pressure gradients and/or internal tidal wave Stokes's drift. In the centre of the shelf this advection is responsible for 25% of the increase in bottom water nitrate seen between April and November 2014. The remaining nitrate increase suggests that about 50–62% of the nitrogen fixed into organic material during spring, summer and autumn phytoplankton growth is recycled in the bottom water over the 12 months between March 2014 and March 2015. In winter, when the water column is vertically mixed, there is a weak net off-shelf transport of about  $1 \text{ m}^2 \text{ s}^{-1}$ , possibly driven by a reversal of the horizontal density gradient caused by excess cooling of shallower shelf waters. Overall, shelf nitrate concentrations are maintained by a combination of riverine supply, recycling of organic material, and summer on-shelf transports. We suggest that the main driver of inter-annual variability in pre-spring nitrate concentrations is variability in the depth of the winter mixed layer over the shelf slope.

### 1. Introduction

Compared to their relatively small size, continental shelves are highly productive regions. Despite accounting for only 9% and 0.5% of the ocean's area and volume respectively (Simpson and Sharples, 2012), it is estimated that ~20% of the global ocean annual primary production takes place on continental shelves (Behrenfeld et al., 2005; Jahnke, 2010). Globally, rivers supply about 1.6 Tmol of dissolved inorganic nitrogen (DIN:  $\text{NO}_2$ ,  $\text{NO}_3$  and  $\text{NH}_4$ ) per year with about 25% of this thought to be used by biogeochemical processes on the shelf (Sharples et al., 2017). However, DIN supplied from rivers is generally low compared to oceanic input. The open ocean is generally viewed as the dominant source of nutrients to the shelf, supplying between 85 and 90% of the nitrogen and 56–58% of the phosphorus required by shelf seas (Liu et al., 2010).

For a wide continental shelf sea it is unclear how nutrients supplied at the coastal and ocean boundaries are transported into the interior of the shelf to drive primary production. The concept of a 'down-welling circulation' as a mechanism for driving the continental shelf pump (Holt et al., 2009), where waters enter the shelf at the surface and leave at depth, is able to account for the export of carbon off-shelf but does not provide a physical means of nutrient supply to bottom waters. The

nutrient distribution along and across a shelf will be controlled by the particular seasonal dynamics of the shelf (e.g. Liu et al., 2000; Roughan and Middleton, 2002). The question we address here concerns how nutrients supplied either at the open ocean or coastal boundaries of a wide, temperate shelf system are able to penetrate into the interior of the shelf sea to support the regular seasonal high primary production (e.g. Hickman et al., this issue; Seguro et al., this issue).

The focus of this study is the Celtic Sea (Fig. 1), an approximately 500 km wide section of the Northwest European Shelf (Huthnance et al., 2009). It is supplied with low salinity water from the Bristol Channel (Uncles, 1984; Hydes et al., 2004), as seen in Fig. 1, and is connected to the deep Northeast Atlantic Ocean across a steep shelf edge. The hydrography of the Bristol Channel is mainly linked to seasonal variability in the riverine flows (e.g. Uncles, 2010). Winter is the wettest season in the region (Pingree, 1980) and the freshwater flow into the Bristol Channel is a maximum during this period (Uncles and Radford, 1980; Uncles, 2010). The shallow water depth and strong tidal currents within the Bristol Channel ensure that the water column is mixed throughout the year (Uncles, 2010). During the summer near the mouth of the Bristol Channel, freshwater may contribute to 50% of the buoyancy input (Brown et al., 2003; Young et al., 2004). Beyond the mouth, the fresher waters strengthen horizontal gradients in the

\* Corresponding author.

E-mail address: [Eugenio.Ruiz@liverpool.ac.uk](mailto:Eugenio.Ruiz@liverpool.ac.uk) (E. Ruiz-Castillo).

<https://doi.org/10.1016/j.pocean.2018.07.006>

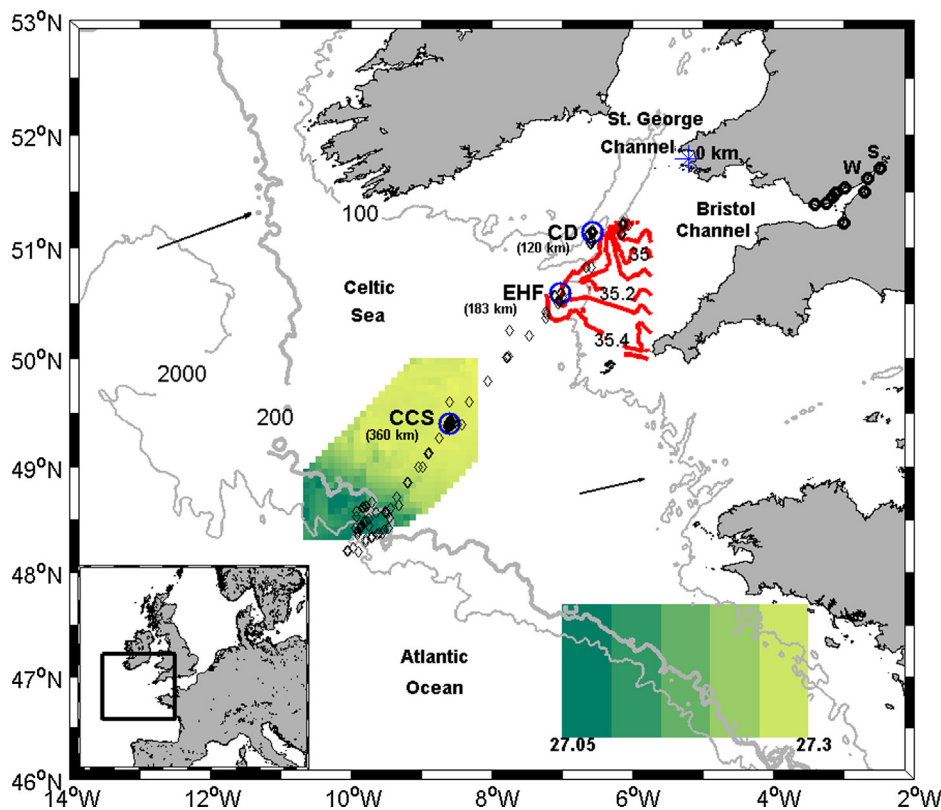


Fig. 1. Map of the Celtic Sea. Black diamonds show the location of CTD casts. Black circles indicate the location of rivers discharging into the Bristol Channel where nutrient data was available. S and W stand for the Severn and Wye Rivers, respectively. The blue asterisk is the reference used in the hydrographic sections. Locations of the Celtic Deep (CD), East of Haig Fras (EHF) and Central Celtic Sea (CCS) moorings are marked by blue circles and in parenthesis distance to the blue asterisk. The density at 75 m between the shelf edge and central shelf is based on interpolation of 8 towed undulating CTD transects in June 2010. Red contours, every  $0.1 \text{ g kg}^{-1}$ , are the surface salinity in May 2015 constructed from the ships underway sampling. Vectors indicate the average wind speed ( $4.41 \text{ m s}^{-1}$  in the north and  $3.06 \text{ m s}^{-1}$  in the south) from 1st January 2014 to 31st December 2015 from Era-interim data. (For interpretation of the references to colour in this figure legend, the reader is referred to the web version of this article.)

northern Celtic Sea (Brown et al., 2003; Young et al., 2004). However, the buoyant low salinity water from the Bristol Channel is mainly diverted northward by the effect of the Earth's rotation, so its influence across the wider Celtic Sea to the south is likely to be limited. In contrast, it has been inferred that high salinity water from the Atlantic Ocean makes its way across the Celtic Sea and into St. Georges Channel (e.g. Hydes et al., 2004; Bowers et al., 2013). Thus, the Celtic Sea is a wide transition zone where oceanic waters with initially high salinity are gradually diluted as they progress northwards, eventually entering the Irish Sea (Brown et al., 2003; Gowen and Stewart, 2005).

Away from the influence of the Bristol Channel, the Celtic Sea is a typical temperate shelf system, where the seasonal changes in water column structure are governed by a competition between surface heating and vertical mixing, the latter formed by varying contributions from tidal currents, wind stress and convective mixing (e.g. Simpson, 1981). In winter, convection (surface heat loss), the tide, and enhanced winds vertically mix the water column. In spring vertical stratification begins once the rate of heating is able to overcome the ability of tidal and wind mixing in redistributing the heat. This seasonally-stratifying region is bounded to the north by the Irish Sea. Most of the Irish Sea remains fully mixed all year, due to shallow water and strong tidal currents, with a tidal mixing front in St. Georges Channel separating the Irish Sea from the stratified Celtic Sea in summer (Simpson, 1976; Horsburgh et al., 2000). East of the Celtic Sea is the English Channel with relatively high salinity originating from the North Atlantic Ocean via the Celtic Sea (Uncles and Stephens, 2007).

To the south and west the Celtic Sea is bounded by the shelf edge and the adjacent Northeast Atlantic Ocean. The shelf edge and slope region guide a slope current of generally salty water (Pingree and Le Cann, 1989; Holt et al., 2009), with strong internal mixing over the 200 m isobath caused by a breaking internal tide during the stratified season (New, 1988; New and Pingree, 1990).

In this paper we demonstrate that seasonality in the outflow from the Bristol Channel combined with the high salinity boundary of the Northeast Atlantic Ocean set up cross-shelf gradients in density that

drive shelf-wide circulation and important cross-shelf transports. We show that despite the dilution of riverine water, the rivers supply an important fraction of the nutrients to the Celtic Sea. However, we find that the nutrients available to each year's spring bloom are a combination of ocean-supplied nutrients and recycled material from the previous year.

## 2. Methods

We combine hydrographic and nutrient data collected by the UK Shelf Sea Biogeochemistry (SSB) Programme (Sharples et al., this issue) along with river flow and nutrient time series from tributaries of the Bristol Channel to build a seasonally resolved understanding of shelf-scale density distributions, circulation and nutrient transports.

### 2.1. CTD transects

Hydrographic data were collected between March 2014 and August 2015 during 9 oceanographic cruises on board the ships RRS *Discovery* and RRS *James Cook*. On each cruise a Seabird 911plus CTD (Conductivity, Temperature and Depth) system collected full water column profiles of temperature, conductivity and pressure. Raw data was processed onto a 1 db grid using standard Seabird Data Processing Software and customized quality control routines. Derived salinity was subsequently calibrated against in situ samples analysed on a Guildline Autosal salinometer. The TEOS-10 functions (IOC et al., 2010) were used to derive thermodynamic properties. A total of 315 CTD casts were performed along the track shown in Fig. 1, and used to construct cross-shelf sections of conservative temperature, absolute salinity and potential density during each cruise. The main cross-shelf CTD transect was set orthogonal to the shelf edge and the general slope of the continental shelf. Spatial interpolation of bottom water density measurements made from a towed undulating CTD package in June 2010 across a 284 km by 146 km area (Fig. 1) also confirmed that the transect was orthogonal to the typical orientation of bottom water isopycnals. The

distance along each hydrographic transect is measured from the eastern side of St. Georges Channel, north of the Bristol Channel mouth (blue asterisk at 51.79°N, 5.2°W; 0 km in Fig. 1). The distance between CTD stations was on average 25 km and a minimum of 5 km, much greater than (on average), or as a minimum equal to the spatial scale of semi-diurnal tidal excursions in the Celtic Sea (Polton, 2015). Although each CTD transect was typically completed over 2–4 weeks, given our focus on low frequency and seasonal variability each transect was assumed to be a synoptic picture of that month. Evolution of the hydrographic structures was consistent with the long-term mooring time series of velocity and hydrography, described later in Section 2.4, confirming that each transect represents a synoptic picture on the time scales of interest. The coarser spatial resolution of the sampling in March 2014 and 2015 on the shelf, between 250 km and 450 km distance from the coast, was augmented by using surface temperature and (calibrated) salinity data (from 6 m depth) recorded continuously along the ship's path. The water column is vertically mixed during these months (Huthnance et al., 2001; Whisgott et al., this issue), therefore the surface temperature and salinity values are representative of the whole water column.

Absolute salinity is used as a conservative tracer to track the movement of the waters in the Celtic Sea. The 35.2 and 35.7 g kg<sup>-1</sup> isohalines were used to identify the influence of fresher water from the Bristol Channel and high salinity Atlantic Water, respectively. In previous studies around the Bristol Channel mouth and south of St. Georges Channel (e.g. Brown et al., 2003) salinities below 35 have been used to describe waters from river origin. In this research the salinity chosen (< 35.2 g kg<sup>-1</sup>) to represent the fresher water influence is based on the new equation of state (IOC et al., 2010), where Absolute Salinity shows an increase of about 0.17 units compared to practical salinity.

## 2.2. CTD nutrient data

Water samples were collected on average from 6 depths between the surface and near bed on each CTD cast and analyzed onboard for dissolved inorganic nutrients using a 5-channel Bran and Luebbe AAI segmented flow auto-analyser following the molybdenum blue method. For further details can be found in Woodward (2016) and Poulton et al. (this issue). Our focus here is on nitrite (NO<sub>2</sub>) plus nitrate (NO<sub>3</sub>) (referred to for the rest of this paper as nitrate), with nitrogen generally being the limiting nutrient for new primary production in this system (Holligan et al., 1984; Pemberton et al., 2004; Davis et al., 2014).

Supported by measurements taken during the cruises (e.g. Garcia-Martin et al., this issue; Poulton et al., this issue; Hickman et al., this issue), we assume that nitrate at 80 m depth, i.e. below the seasonal pycnocline and much deeper than the Euphotic zone (1% light level is 46 m), is largely unaffected by phytoplankton consumption, and therefore nitrate can be considered a quasi-conservative tracer. The nitrate-salinity relationship from March 2014 was used as the pre-spring bloom state of shelf nitrate distributions, and to provide estimates of the physical transport of nitrate in bottom waters at CCS throughout the rest of the stratified period of the year by tracking the movement of isohalines. Subsequent increases in bottom water nitrate concentrations above the values estimated from the conservative behavior based on the March nitrate-salinity relationship are then assumed to indicate addition of deep shelf water nitrate by regeneration of organic material.

## 2.3. River discharge and nutrient load

Daily river flow data, provided by Natural Resources Wales and the National River Flow Archive, from 33 tributaries that discharge into the Bristol Channel were added together to quantify the total freshwater input into the Bristol Channel between the 1st of July 2013 and the 30th of September 2015. After analysing the hydrographic data, the Bristol Channel was identified as the main source of fresher water;

therefore only tributaries that discharge directly into the channel were considered (Fig. 1). Although data were not available for all, the Severn and the Wye Rivers are included which are the main freshwater suppliers accounting for about 54% of the total input of freshwater (Uncles and Radford, 1980; Jonas and Millward, 2010).

Time series data provided by Cefas (courtesy of Dr. Sonja van Leeuwen) were used to assess the total inorganic nitrogen (NH<sub>4</sub>, NO<sub>2</sub> and NO<sub>3</sub>) input into the Bristol Channel from 9 tributaries (black circles in Fig. 1). Water samples were analysed for NH<sub>4</sub>, NO<sub>2</sub> and TON (Total Oxidised Nitrogen) using a Konelab discrete analyser at the National Laboratory Service (<http://natlabs.co.uk>). NO<sub>3</sub> was then calculated from TON and NO<sub>2</sub> (TON – NO<sub>2</sub> = NO<sub>3</sub>). NH<sub>4</sub> is not included in CTD nutrient data.

As reported in Jonas and Millward (2010) the contribution to the total inorganic nitrogen load made by each tributary scales with their freshwater discharges. Of the total inorganic nitrogen input supplied by the 9 tributaries summed here, the Severn and Wye Rivers account for 43% of the 2013–2014 winter total. Additional contributions from the Bristol Avon, Cadoxten, Parrett, Rhymney, Taff, Thaw and Usk, many of which are identified as significant contributors to both the freshwater and total inorganic nitrogen load by Jonas and Millward (2010) are also accounted for. Data in the period between the 1st of October 2013 and the 30th of September 2014 are used here.

## 2.4. Moorings

Salinity time series from moorings located in the central Celtic Sea (CCS) and the Celtic Deep (CD) (Fig. 1) were available with temporal resolutions of 5 and 30 min respectively (Whisgott et al., 2016; Hull et al., 2017). The surface salinity time series at CD was collected between the 23rd March 2014 and the 8th July 2015. At CCS two salinity time series were used to compare the hydrographic conditions in the upper and bottom layers, at 20 m and 120 m below the sea surface, between the 26th March 2014 and the 23rd of August 2015. The salinities were calibrated against in situ samples analysed on a Guildline Autosol Salinometer with a stated accuracy of < ± 0.002 psu. All three salinity time series were filtered using a low-pass Lanczos filter (Thompson and Emery, 2014) with a cut-off frequency of 1/24 h<sup>-1</sup>, so only fluctuations with periods longer than 1 day were considered.

ADCP velocity time series at CCS, Celtic Deep and at a site referred to as East of Haig Fras (Fig. 1) are used to assess the speed and direction of bottom water currents. Near full water column velocity time series were available at CCS between the 22nd June 2014 and the 25th July 2015, with a 57 day gap during early summer 2014 (Whisgott et al., 2018). Velocities were recorded in 2.5 m vertical bins between 7.5 m and 127.5 m above the seafloor (mean total water depth of 147 m), over 2.5 min ensembles. At East of Haig Fras (EHF) and at the Celtic Deep, velocities were recorded every hour within the bottom 40 m of the water column only, at a vertical resolution of 0.5 m (Thompson et al., 2017, 2018). Data was successfully returned at EHF from 22nd March 2014 to 24th October 2014 and then from 17th March 2015 to 30th August 2015. At the Celtic Deep velocities were recorded from autumn 2014 until spring 2015 (23rd October 2014 to 8th May 2015), with a short 22 day gap starting mid-February 2015.

A depth mean of the instantaneous velocities within the bottom 40 m of the water column at all sites was calculated. Temporal averaging was then performed within a moving window of twenty M<sub>2</sub> tidal periods (10.3 days). These time series reveal the net movement of near bottom water across the shelf on an approximate 10 day time scale and are used to independently support the estimates of transport inferred from the movement of isohalines across the shelf.

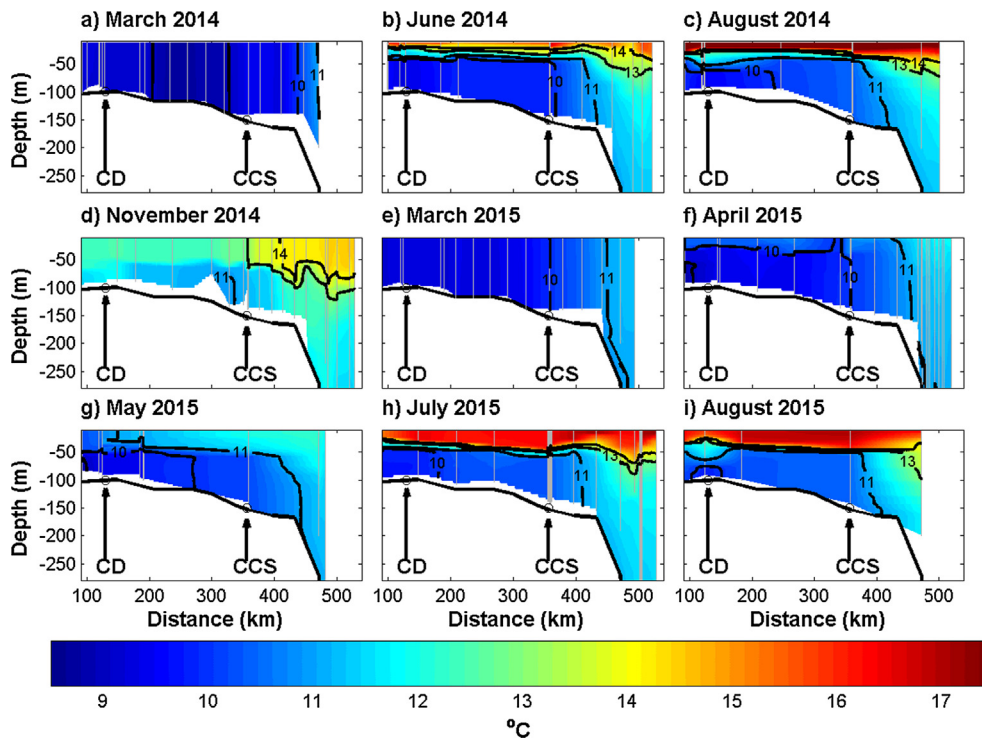


Fig. 2. Conservative temperature sections across the Celtic Sea. Vertical gray lines indicate the location of the CTD casts. Gray circles at the bottom show the position of the moorings at Celtic Deep (CD) and the central Celtic Sea (CCS).

### 3. Results

#### 3.1. Shelf-wide seasonal hydrography

In March 2014 and 2015 the Celtic Sea was vertically mixed with cross-shelf horizontal gradients in conservative temperature (Fig. 2a and e). Relatively cold waters with values below  $10^{\circ}\text{C}$  were located over the central Celtic shelf while slightly warmer waters were located near the shelf break. In April and May 2015 the water column gained heat and the upper 30 m warmed up across the entire shelf (Fig. 2f and g). A two-layer system had developed by May (Fig. 2g) with a weak thermocline at a depth of about 50 m separating upper and lower layers with temperatures of  $11.5^{\circ}\text{C}$  and  $10^{\circ}\text{C}$  respectively. Throughout summer, June to August (Fig. 2b, c, h, and i), vertical thermal stratification strengthened. Maximum near surface temperatures of  $16^{\circ}\text{C}$  occurred in August (Fig. 2c and i). In autumn, November (Fig. 2d), the thermocline deepened below 50 m, as the surface layer cooled and generated convective vertical mixing. Throughout the year water near the shelf break (approximately 450 km; depth of 200 m) remained warmer than bottom water across the rest of the shelf, probably because of the along-slope flow of warmer waters originating from more southerly latitudes as well as strong internal tidal mixing acting to redistribute heat vertically.

In March 2014 and 2015 the vertical isohalines across the whole shelf reflected the vertically well-mixed, isothermal conditions (Fig. 3a and e). A horizontal cross-shelf salinity gradient was maintained between the low salinity input of the Bristol Channel in the north and the high salinity ( $> 35.7 \text{ g kg}^{-1}$ ) oceanic water near the shelf edge. In April 2015 (Fig. 3f) a band of low salinity water ( $35.2 \text{ g kg}^{-1}$ ) was observed in the northern Celtic Sea and remained within 100–150 km of St. Georges Channel. The  $35.2 \text{ g kg}^{-1}$  isohaline was vertically sheared, with lower salinity water extending further offshore above the thermocline. Noting that isohalines during the previous winter were vertical, this suggests an offshore transport of low salinity surface water. Through late spring and summer of both years (Fig. 3b, c, g, h, and i) this suggestion of differential transport between surface and bottom

layers strengthened, with marked shear also observed in the  $35.4$  and  $35.45 \text{ g kg}^{-1}$  isohalines further out across the central shelf.

The salinity of bottom water across the Celtic Sea increased from March into late autumn (Fig. 4a). Between March and August 2014, the  $35.6 \text{ g kg}^{-1}$  isohaline at the sea bed moved from the shelf edge to just beyond CCS, a distance of approximately 100 km. This isohaline was initially vertical in March, but sheared in August, suggesting a persistent on-shelf transport of bottom water over the summer and autumn months. In 2015 the  $35.6 \text{ g kg}^{-1}$  isohaline did not move as far. Instead, evidence of on-shelf bottom water transport is found in the  $35.5 \text{ g kg}^{-1}$  isohaline that moved 120 km onshore between March and August 2015. In 2014 and 2015 the mean onshore flows inferred from this movement in salinity were about  $1 \text{ km day}^{-1}$  (Fig. 4b). Maximum velocities above  $1.5 \text{ km day}^{-1}$  occurred in November 2014 and August 2015.

The ingress of more saline oceanic water onto the shelf beneath the thermocline and the offshore spread of fresher water above it ensured that much of the Celtic Sea was vertically stratified in salinity as well as temperature throughout the summer.

Between November 2014 and March 2015 there is an indication of water moving from mid-shelf towards the outer shelf and shelf edge. All isohalines in November 2014 make some progress towards the shelf edge (Fig. 3d and e). A consistent off-shelf movement occurred ( $0.8 \text{ km day}^{-1}$ ) from December 2014 to April 2015 (Fig. 4b) of bottom water salinity as a part of the broader seasonal cycle of salinity variations (Fig. 4). However, the extent of the apparent movement will be altered due to vertical mixing from mid-December through to March (Fig. 4a).

Together, the temperature and salinity structures determined the vertical and horizontal density gradients across the Celtic Sea (Fig. 5). From May to August (Fig. 5b, c, g, h, and i) the bottom-surface density difference across most of the shelf was 1 to  $1.2 \text{ kg m}^{-3}$ . June, July and August were the most strongly stratified (Fig. 5b, h and i). The pycnocline, over both the shelf and the deep ocean, was defined by the  $1026.8$  and  $1027 \text{ kg m}^{-3}$  isopycnals. The development of a low salinity surface plume in April 2015 (Fig. 5f) once weak vertical thermal stratification had started was reflected in a 30–40 m thick anomalously low

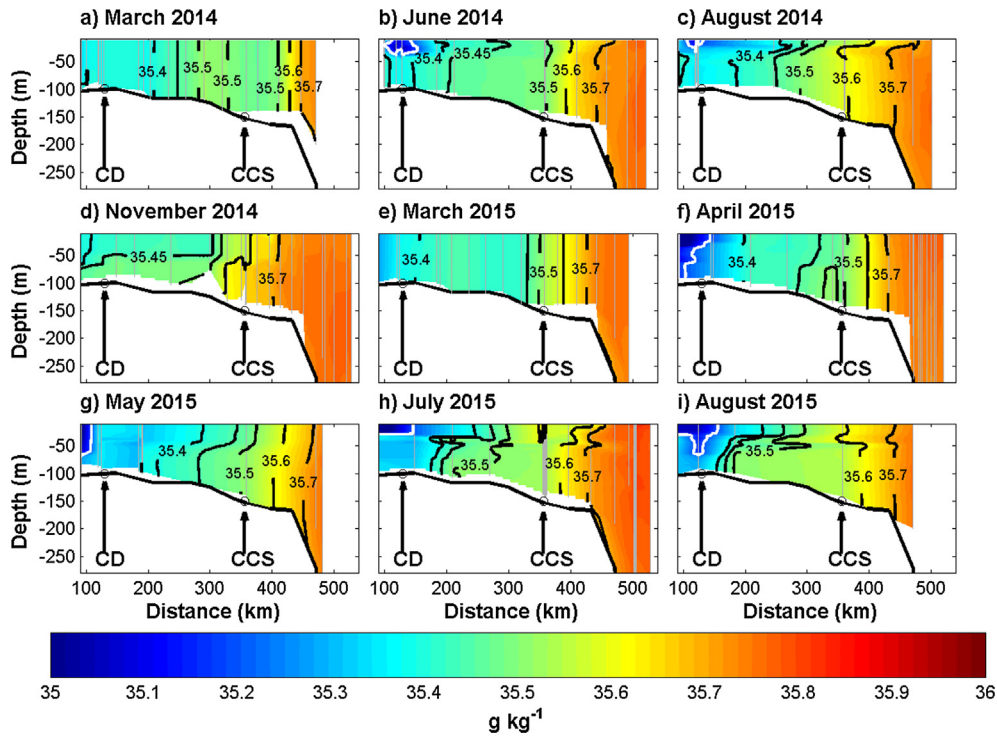


Fig. 3. Absolute salinity sections across the Celtic Sea. CTD casts and mooring locations marked as per Fig. 2. White contours represent the  $35.2 \text{ (g kg}^{-1}\text{)}$  isohaline that indicates the presence of fresher water.

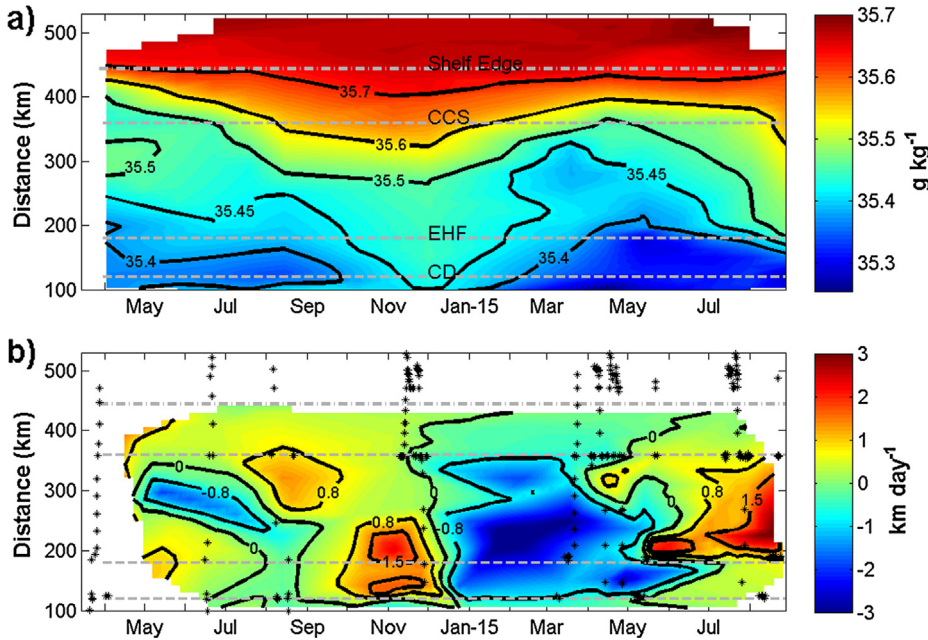


Fig. 4. (a) Bottom water absolute salinity (at 80 m) along the CTD transect and (b) velocities calculated from the isohaline displacement along the CTD transect. Gray dashed lines show the location of CD, EHF and CCS. Location of the shelf break is represented by -.- gray line. Black asterisks in (b) indicate where CTD casts were carried out.

density surface layer in the north of the Celtic Sea.

Beneath the pycnocline there were important cross-shelf gradients in bottom water density (Fig. 6). Throughout the year, the bottom water density from CCS towards the shelf-edge typically decreases; this gradient intensifies during the latter half of the summer and into autumn as water at the shelf edge becomes increasingly warmer compared to the central shelf. Moving on-shelf from CCS towards the coast there is also a general decrease in density with a persistent mid-shelf maximum in bottom water density varying seasonally between about 200 and 350 km from the northern end of the transect line.

### 3.2. Near bed ADCP velocities

The direction and magnitude of near bed velocities recorded at CCS, East of Haig Fras (EHF) and at the Celtic Deep (CD) are supportive of the direction and magnitude of flows inferred from the movement of isohalines (Fig. 7). During April at CCS there was on average a  $1 \text{ km day}^{-1}$  current directed increasingly on-shelf in the bottom 40 m of the water column (Fig. 7a). At the end of April strong, on-shelf north-eastward velocities of  $1.8 \text{ km day}^{-1}$  were recorded. Much weaker on-shelf flows were observed at CCS throughout July and early August, in agreement with the  $0(0.5 \text{ km day}^{-1})$  velocities predicted from the

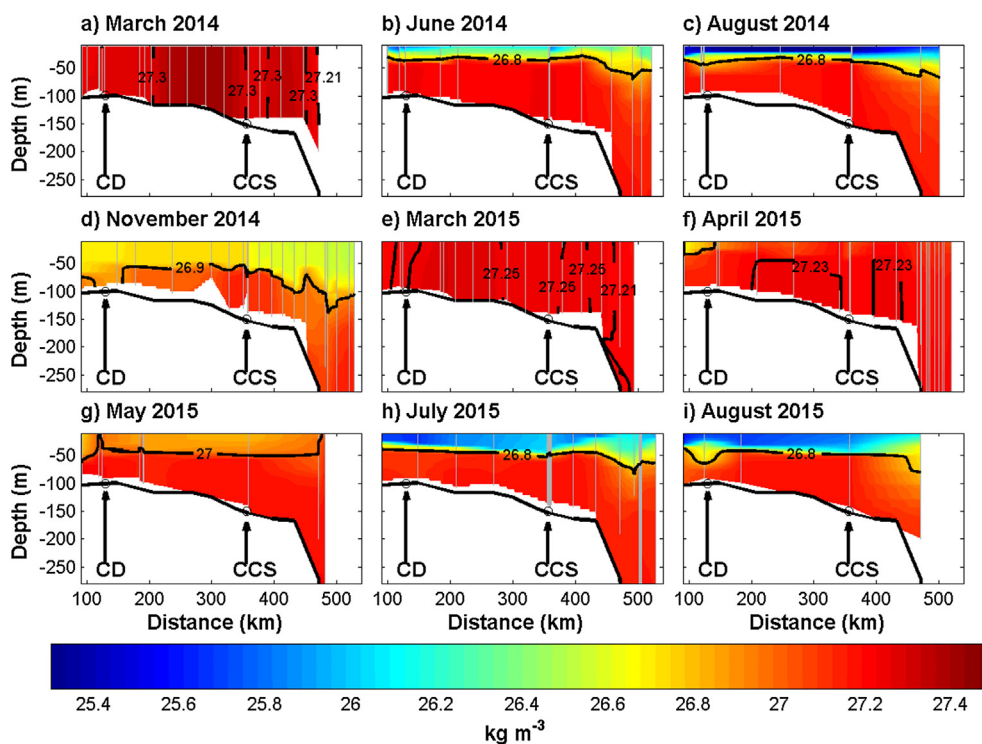


Fig. 5. Potential density sections across the Celtic Sea. CTD casts and mooring locations marked as per Fig. 2.

isohaline movement (Fig. 4b). During the second half of August, however velocities increase to on average  $1.7 \text{ km day}^{-1}$  and the current turns towards the northeast (on-shelf), the timing of which is consistent with the predicted increase in on-shelf flow at this time (Fig. 4). Throughout September, October and early November episodes of opposing strong ( $1\text{--}3 \text{ km day}^{-1}$ ) on-shelf and off-shelf flow occur. The net result is a weak ( $0.1 \text{ km day}^{-1}$ ) east-northeast flow, which is supportive of the reduced on-shelf movement of isohalines over this period at CCS. Isohaline movements at CCS during 2015 predict on-shelf transport from May onwards, increasing to  $0.8 \text{ km day}^{-1}$  in early August 2015

(Fig. 4b). Bottom currents from the ADCP at CCS average  $0.6 \text{ km day}^{-1}$  north-east, directly on-shelf between 1st May 2015 and the end of July 2015.

As is observed at CCS, the latter half of April 2014 at Haig Fras is dominated by strong on-shelf bottom water flows, peaking at  $3 \text{ km day}^{-1}$  (Fig. 7b). The predicted off-shelf movement during August 2014 (Fig. 4b) is supported by a period of sustained  $0.5 \text{ km day}^{-1}$  off-shelf flow recorded by the ADCP at Haig Fras. In 2015 the latter stages of significant off-shelf winter transport at Haig Fras estimated from the isohaline displacement is supported by an average flow of  $1.2 \text{ km day}^{-1}$

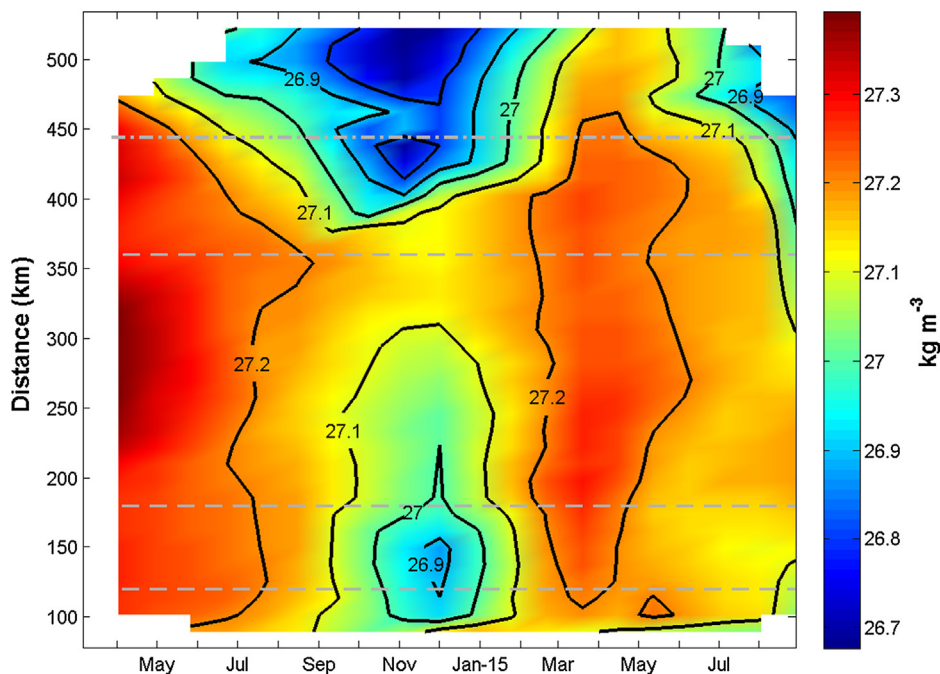
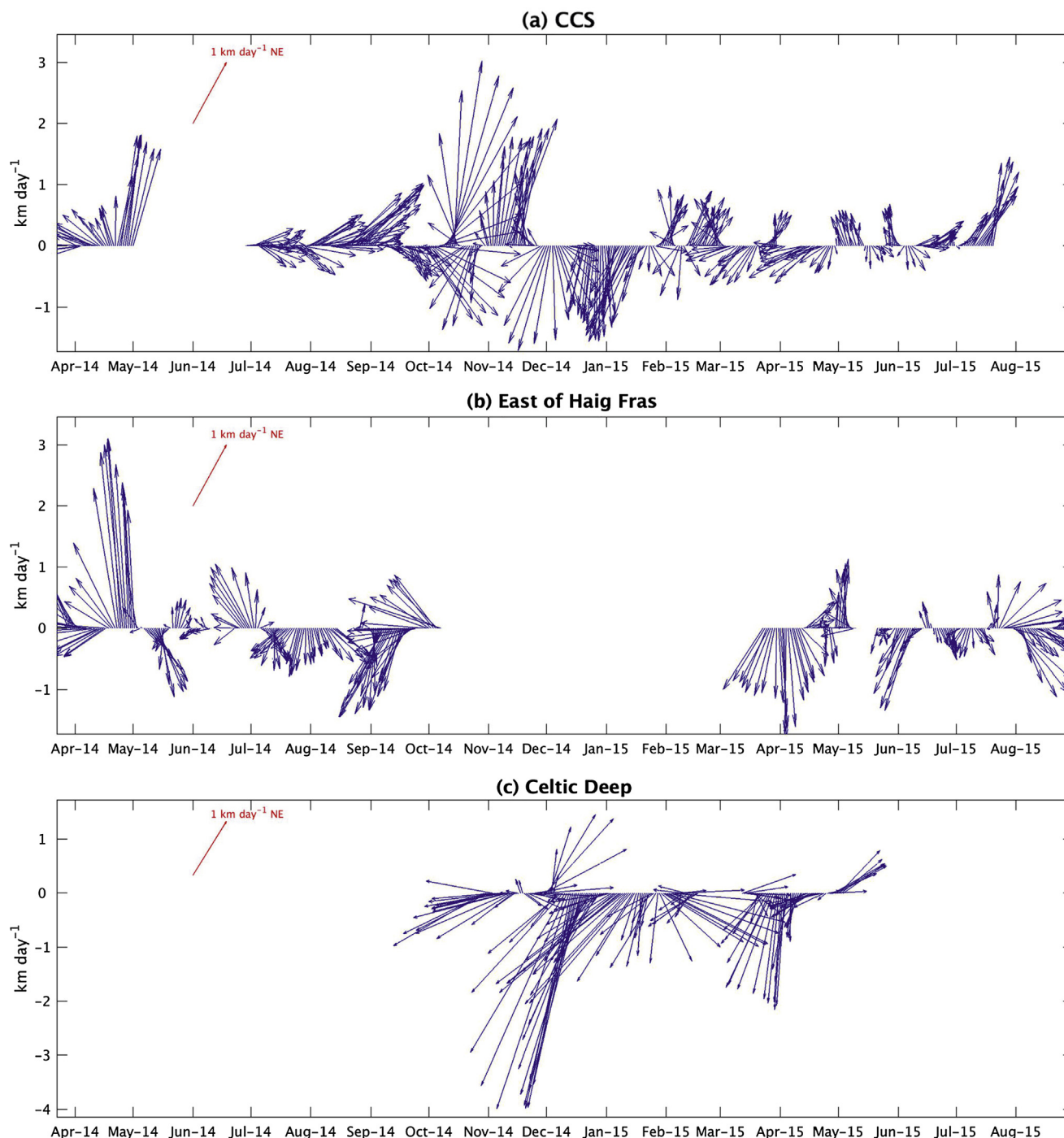


Fig. 6. Bottom water density (at 80 m) along the CTD transects. Shelf edge, CD, EHF and CCS locations indicated as per Fig. 4a.



**Fig. 7.** Mean velocities within the bottom 40 m of the water column at (a) CCS, (b) East of Haig Fras and (c) Celtic Deep. At each location, the instantaneous velocities were averaged within a running window of  $20 \times M_2$  tidal periods (10.3 days). For clarity, one vector every 24 h is plotted. Note that panel (c) has a different vertical scale.

southward between 22nd March and 13th April 2015.

The ADCP record at CCS over the winter months confirms the anticipated off-shelf movement of bottom water. Between the 26th November 2014 and 26th January 2015 the bottom water currents averaged  $0.9 \text{ km day}^{-1}$  towards the south (Fig. 7a). During the remainder of the well mixed period at CCS bottom water currents oscillated between being on- and off-shelf, suggesting that the majority of the off-shelf transport over the outer shelf likely occurred during early winter, a detail that is reflected by the sharp decrease in bottom water salinity recorded during December 2014 at CCS (Fig. 8c). Further on-shelf at the Celtic Deep near bed currents over the winter were stronger

and more persistently off-shelf (Fig. 7c), averaging  $1.2 \text{ km day}^{-1}$  southwest between 5th December and 1st May 2015, and in agreement with the greater cross-shelf displacements estimated for lower value isohalines.

### 3.3. River flow, nutrient and salinity time series

River discharge into the Bristol Channel was greatest during winter (Fig. 8a). Maximum flows of  $1800 \text{ m}^3 \text{ s}^{-1}$  and  $1200 \text{ m}^3 \text{ s}^{-1}$  were reached during the winters of 2013/2014 and 2014/2015, respectively. Relatively high discharge was sustained throughout most of the 2013/

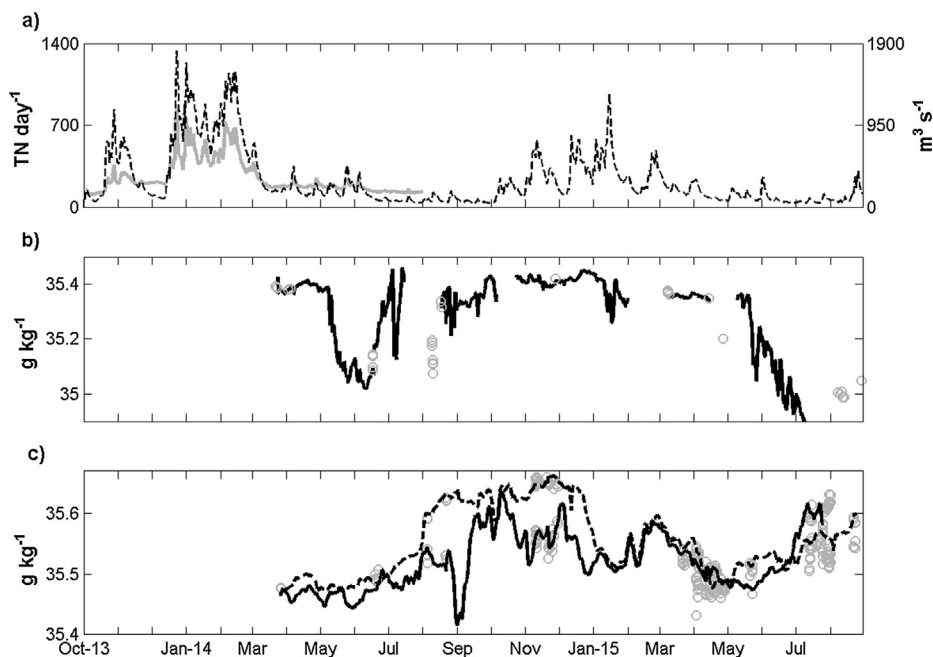


**Fig. 8.** (a) River discharge in  $\text{m}^3 \text{s}^{-1}$  (dashed line) and nutrient input in Tonnes of Nitrogen per day $^{-1}$  (gray) into the Bristol Channel. Peak winter river discharge occurs on 23rd December 2013 and 15th January 2015. (b) Surface salinity at the Celtic Deep mooring (solid line). Following peak river discharge the salinity starts to decrease on 6th May 2014 and 13th May 2015. (c) Surface (20 m, solid line) and near bottom (140 m, dashed line) salinity at the central Celtic Sea (CCS) mooring. Open gray circles in (b) and (c) are the salinities measured independently from the CTD during the cruises and validate the quality of the salinity time series at each mooring.

2014 winter period (December to March), whereas 2014/2015 was characterized by a series of smaller peaks (below  $950 \text{ m}^3 \text{ s}^{-1}$ ) from October onwards. After March, the river discharge decreased significantly and remained low throughout spring and summer.

The total nitrogen supply into the Bristol Channel is strongly correlated with the freshwater discharge (Fig. 8a) with a Pearson correlation coefficient ( $R^2$ ) of 0.97. Maximum input was during winter with peak values above 700 tonnes of nitrogen day $^{-1}$ , decreasing to values below 200 tonnes of nitrogen day $^{-1}$  in spring and summer. We can make an estimate of the nitrate contribution from rivers by assuming that the total nitrogen (the sum of nitrate, nitrite and ammonium) indicates the potential nitrate as the nitrogen enters the coastal sea. Taking a mean winter discharge rate of  $1200 \text{ m}^3 \text{ s}^{-1}$ , or  $1 \times 10^8 \text{ m}^3 \text{ day}^{-1}$ , combined with a mean total nitrogen load of 550 tonnes per day suggests that the freshwater nitrate concentration during the winter preceding spring 2014 was about  $390 \text{ mmol m}^{-3}$ .

At the Celtic Deep, in the northern Celtic Sea, the surface salinity dropped from  $35.4 \text{ g kg}^{-1}$  in early May to  $35 \text{ g kg}^{-1}$  in mid-June 2014 (Fig. 8b). A pronounced  $0.4\text{--}0.5 \text{ g kg}^{-1}$  decrease in salinity also started in mid-May 2015 and continued until the end of the record (July 2015). For context, the range in surface water salinity experienced over a spring tidal cycle at the Celtic Deep is  $0.03 \text{ g kg}^{-1}$  an order of magnitude less than the May decrease. These trends are consistent with the perspective provided by the CTD transects (Fig. 3) and support the idea of low salinity water spreading out over the northern Celtic Sea. Throughout the latter half of summer 2014 the surface salinity at the Celtic Deep increased and remained around values of  $35.4 \text{ g kg}^{-1}$  from October onwards.

In the central Celtic Sea the bottom water salinity increased over the summer and reached a maximum in November/December (Fig. 8c). A pattern that is again consistent with the seasonal hydrographic sections and which we interpret as indicating a near-bed transport of high salinity water across the shelf. Sustained periods of time between July 2014 and January 2015, where the top to bottom salinity difference was  $0.05\text{--}0.1 \text{ g kg}^{-1}$ , reveal prolonged episodes of vertical salinity stratification on the central shelf.

### 3.4. Nitrate distribution across the Celtic Sea

The distribution of nitrate across the shelf is shown in Fig. 9. During both March 2014 and March 2015 (Fig. 9a and e), when the water

column was vertically well mixed, nitrate was also homogeneously distributed throughout the water column. Across the shelf there was a horizontal nitrate gradient with higher concentrations at the shelf edge ( $8\text{--}9 \text{ mmol m}^{-3}$ ) decreasing to about  $6 \text{ mmol m}^{-3}$  in the Celtic Deep. Following the onset of stratification in April (Fig. 9f), nitrate concentrations rapidly reduced to zero in the surface layer due to uptake by primary producers (Garcia-Martin et al., this issue; Poulton et al., this issue). The surface layer remained depleted of nitrate until the onset of surface layer deepening arising from convective and wind-driven mixing in autumn (Wihsgott et al., this issue). It is clear that convection entrained deep-water nutrients up into the autumnal (Fig. 9d, November 2014) surface layer where nitrate reached  $2\text{--}3 \text{ mmol m}^{-3}$ .

In April 2015 (Fig. 9f), early spring, the bottom water nitrate concentration across the shelf was  $6 \text{ mmol m}^{-3}$ . A higher pool of nitrate ( $> 8 \text{ mmol m}^{-3}$ ) was located seaward of the shelf-break. A pool of higher bottom water nitrate ( $> 7 \text{ mmol m}^{-3}$ ) was also observed at the northern end of the section, coincident with lower salinity water (Fig. 3f), thought to originate from the Bristol Channel. Throughout the stratified months (Fig. 9b–d and g–i) the bottom water nitrate concentration across the whole shelf increased, typically reaching  $9\text{--}10 \text{ mmol m}^{-3}$  by August. The on-shelf movement of the  $8 \text{ mmol m}^{-3}$  contour between April 2015 and May 2015 (Fig. 9f and g) appears to imply that there was a physical transport across the shelf-break.

## 4. Discussion

Based on the patterns of the isohalines from the CTD sections (Figs. 3 and 4) and the salinity time series at the mooring sites (Fig. 8) the results indicate several important aspects of cross-shelf flows. In particular, (1) offshore surface flow of low density water in the north of the transect in spring, (2) onshore flows of bottom water in the central Celtic Sea and near to the shelf edge during summer, and (3) off-shelf flows of bottom water across the shelf and towards the shelf edge during winter. We will now consider each of these aspects of mean flow to assess the likely driving force and also to consider the consequences for the transports of nutrients. While we lack data to track how the shelf evolved over winter, we can make some assessment of the net changes to the shelf system between November 2014 and March 2015 which are relevant to understand whether or not the shelf receives new nutrients from the ocean during winter. Finally, we will consider the implications for nutrient supplies to the central Celtic Sea.

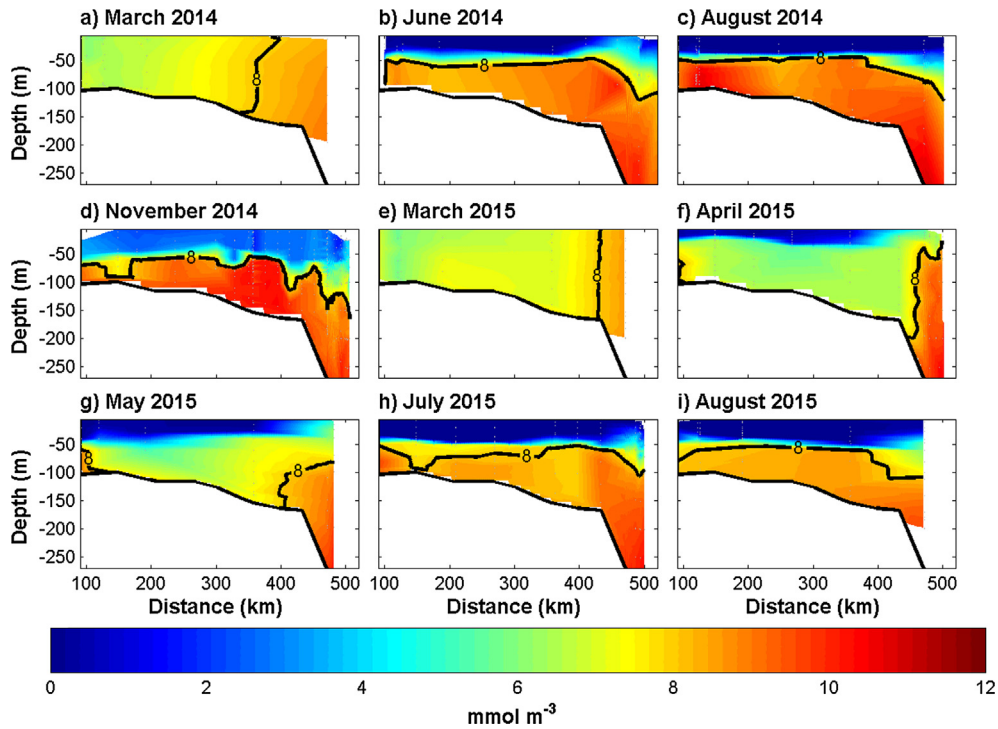


Fig. 9. Nitrate sections across the Celtic Sea. The black line represents the  $8 \text{ mmol m}^{-3}$  contour.

#### 4.1. Surface offshore flow in the northern Celtic Sea

The low density, low salinity water exiting the Bristol Channel has typically been assumed to mainly head north towards the Irish Sea as a buoyancy-driven flow influenced by Coriolis (Uncles, 2010). However, salinity transects (Fig. 3) suggest a gradual freshening in the northern Celtic Sea, and a sharpening of the horizontal salinity gradient, from November 2014 through to April 2015. Riverine input from the southern coast of Ireland into the Celtic Sea is minor and flows westward within a coastal current (Brown et al., 2003). Freshening of the northern Celtic Sea between winter and spring is therefore more likely to be associated with elevated winter discharge from the Bristol Channel.

In April 2015, significant shear in the salinity structure is clear, with a plume-like low-salinity layer in the northern Celtic Sea developed coincident with the thermally-stratified surface layer (Fig. 2). Over most of the Celtic Sea in spring, surface salinity tends to reduce compared to the bottom water, indicating an offshore transport that sets up a haline stratification across the shelf that persists until winter (autumnal) re-mixing. The shear of the  $35.2 \text{ g kg}^{-1}$  isohaline in April 2015 suggests a relative movement of the surface layer offshore by about 35–40 km over the bottom layer. Assuming that this shear must have developed after the March 2015 survey suggests a mean surface layer flow relative to the bottom layer of at least  $1.4 \text{ km day}^{-1}$  ( $1\text{--}2 \text{ cm s}^{-1}$ ). The position of the  $35.2 \text{ g kg}^{-1}$  isohaline stayed roughly constant after this April 2015 event. The speed of the flow, followed by the halt of further offshore progression, suggests initial relaxation of the horizontal density gradient triggered by the spring thermal stratification switching off mixing between surface and bottom waters. This is akin to the ‘estuarine-style’ baroclinic circulation described by Linden and Simpson (1988) for a number of shallow seas and estuaries worldwide. As fresh water from the Bristol Channel is allowed to extend towards the northern Celtic Sea it is continually mixed with (and freshens) surrounding water, a non-reversible process that extends the southward influence of the Bristol Channel.

The width of the surface relaxation should equal a few internal Rossby,  $R_0$ :

$$R_0 = \frac{\sqrt{g \frac{\Delta\rho}{\rho_0} h_s}}{f} \quad (1)$$

where  $g = 9.81 \text{ m s}^{-2}$ ,  $\Delta\rho$  is the bottom-surface density difference ( $\sim 1.0 \text{ kg m}^{-3}$ ),  $\rho_0$  the reference density ( $1027 \text{ kg m}^{-3}$ ),  $f$  the Coriolis parameter and  $h_s$  the surface layer thicknesses of about 40 m. Using these typical values  $R_0$  is  $\sim 5.5 \text{ km}$ . The width of the relaxation is therefore about 7 times  $R_0$  ( $7 \times 5.5 \text{ km} = 38.5 \text{ km}$ ), a scaling that lies within the range of values reported by Sharples et al. (2017) for the width of a fresh water plume. The width of the relaxation will vary depending on the prevailing wind conditions, the strength of the river discharge, the level of tidal mixing and the strength of the existing horizontal salinity gradient. Once the surface plume has reached its maximum southward extent it will feel the effects of rotation and the low salinity water will join the cyclonic geostrophic gyre circulation described by Horsburgh et al. (1998) and Brown et al. (2003).

The potential for nutrient supply from rivers to the Celtic Sea spring bloom can be considered by noting the dilution of the salt content and the initial river nutrient concentration of  $390 \text{ mmol m}^{-3}$  which will be modified by biogeochemical processing during transit from the rivers to the Celtic Sea. An estimate of the transit time of fresh water from the Severn Estuary and Bristol Channel to the Celtic Sea can be made by considering the time between peak river discharge and the sharpening of the horizontal salinity gradient and drop in surface salinity in the northern Celtic Sea. In 2013/2014 the decrease in salinity at the Celtic Deep (on 6th May 2014) takes place 4.5 months after peak river discharge (on 23rd December 2013). In 2014/2015 a drop in salinity at the Celtic Deep starts just 3.5 months after the peak in river input (on 15th January 2015), or a more conservative 4.5 months if the earlier secondary peak in discharge during December 2014 is considered. On average therefore, it takes about 4 months for fresh water to reach the northern Celtic Sea. For context, Uncles and Radford (1980) estimate the residence time of the Severn Estuary (from Maisemore Wier north of Gloucester to Minehead) to be about 100 days (3.3 months) in the winter, a timescale well aligned with the evidence presented here.

A 4 months transit time would imply a mean flow of about  $2\text{--}3 \text{ cm s}^{-1}$ , which is a reasonable value for a mean surface flow in the

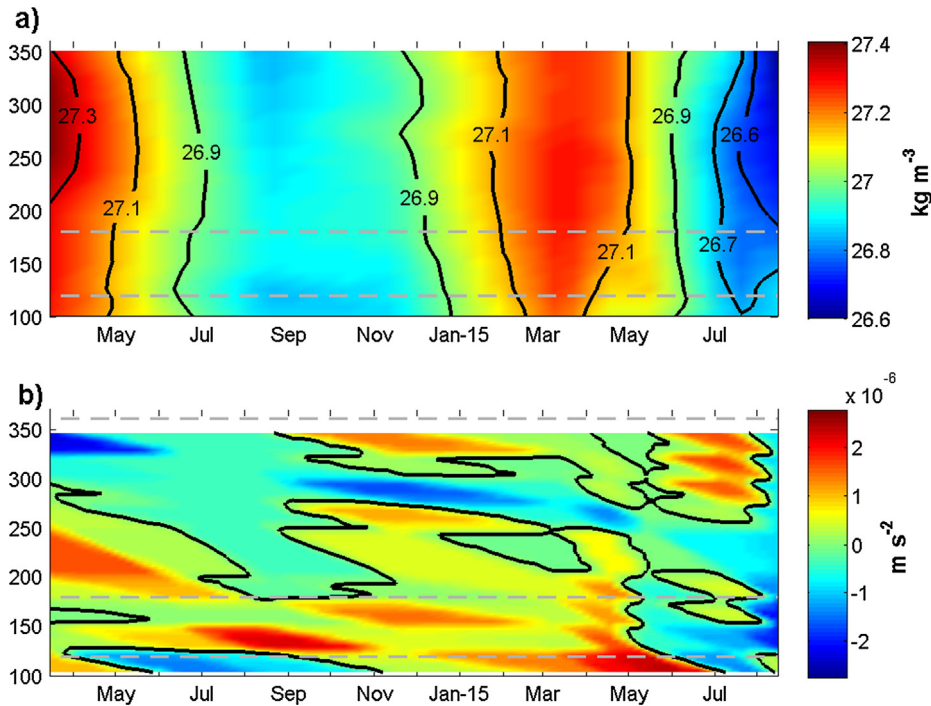


Fig. 10. (a) Depth averaged density across the Celtic Sea between CCS and CD. (b) Pressure gradient across the Celtic Sea. The black contour in (b) represents the  $0 \text{ m s}^{-2}$  pressure gradient. Positive values indicate on-shelf acceleration.

Bristol Channel (Uncles, 2010). Removal of nitrogen by biogeochemical processing over 4 months will reduce the riverine nitrate concentration. Based on data collected from lakes, rivers, estuaries and continental shelves Seitzinger et al. (2006) established a relationship between the removal of DIN (by de-nitrification) from aquatic systems and the residence time of water within them whereby the percentage (%) of DIN removed,  $\text{DIN}_{\text{rem}}$ , is related to the residence time  $T_{\text{res}}$  (months) by  $\text{DIN}_{\text{rem}} = 23.4 T_{\text{res}}^{0.204}$ . This empirical relationship suggests that about 30% of the total riverine nitrate will be removed over 4 months. It is less clear how long the riverine influence would take to reach the CCS mooring site, but assuming 6–12 months, and again using the relationship from Seitzinger et al. (2006) would mean a reduction in the original riverine nitrogen input of between 34% and 40%. Taking the oceanic salinity to be  $35.7 \text{ g kg}^{-1}$ , and the spring salinities in the northern Celtic Sea and at the CCS mooring site to be  $35.4$  and  $35.55 \text{ g kg}^{-1}$  respectively, results in the freshwater fraction to be 0.8% in the north and 0.4% at CCS. Thus the contribution of river nitrate load to the nitrate observed at the Celtic Deep in spring is about  $2.2 \text{ mmol m}^{-3}$  of the observed  $7 \text{ mmol m}^{-3}$ , so about 30% of the nitrate available to the spring bloom in the Celtic Deep is riverine in origin. In the central Celtic Sea, by the CCS mooring site, the same calculation suggests  $0.9\text{--}1.0 \text{ mmol m}^{-3}$  of river-sourced nitrate out of a total of  $8\text{--}9 \text{ mmol m}^{-3}$ , so approximately 10% of the nitrate available to the spring bloom at CCS is riverine.

#### 4.2. On-shelf bottom water flows

In March 2014 the  $35.6 \text{ g kg}^{-1}$  isohaline was situated at the shelf edge. During summer 2014 this water in the bottom layer moved approximately 100 km onto the shelf by August 2014. In spring-summer 2015 the same isohaline remained almost fixed, just 30 km onto the shelf from the shelf edge. The  $35.5 \text{ g kg}^{-1}$  isohaline, initially 25 km on-shelf from CCS, had moved about 120 km further onto the shelf by July-August 2015. Bottom water transports can be estimated by taking the mean flow implied by the isohaline movement and the thickness of the layer. For March to August 2014 the movement of the  $35.6 \text{ g kg}^{-1}$  isohaline (speed approximately  $0.87 \text{ km day}^{-1}$  ( $1 \text{ cm s}^{-1}$ ), layer

thickness 150 m) suggests a transport of  $1.5 \text{ m}^2 \text{ s}^{-1}$ . For March to July 2015, the movement of the  $35.5 \text{ g kg}^{-1}$  isohaline (speed approximately  $0.87 \text{ km day}^{-1}$ , layer thickness 100 m) suggests a transport of  $1 \text{ m}^2 \text{ s}^{-1}$ .

There are several potential mechanisms for driving this bottom water across the shelf. We consider here: (1) horizontal dispersion down the horizontal salinity gradient, (2) a compensating onshore transport for a surface offshore Ekman transport, (3) a mean density-driven (or pressure gradient) transport, (4) the Stoke's drift of an on-shore propagating internal tidal wave, and (5) onshore baroclinic transport of high salinity lenses in the pycnocline (Hopkins et al., 2012).

##### (1) Horizontal dispersion

The timescale for horizontal dispersion can be estimated as  $K_h \frac{\Delta s}{\Delta y}$  where  $\frac{\Delta s}{\Delta y}$  is the horizontal salinity gradient and  $K_h$  is a horizontal dispersion coefficient. Observations of dispersion coefficients in shelf seas are typically  $10\text{--}600 \text{ m}^2 \text{ s}^{-1}$  (Sanders and Garvine, 2001; Houghton et al., 2009). Taking a high value of  $10^3 \text{ m}^2 \text{ s}^{-1}$  suggests a timescale of over 1 year for the observed bottom layer isohaline shifts in 2014 and 2015, much slower than the observed transport.

##### (2) Ekman transport

For the surface Ekman transport we take the mean cross-shelf Ekman transport between March and September 2014 and 2015 calculated as  $\tau_w / \rho_o f$  with  $\tau_w$  the averaged along-shelf edge wind stress ( $0.01$  and  $0.02 \text{ N m}^{-2}$  in 2014 and 2015 respectively),  $\rho_o \sim 1027 \text{ kg m}^{-3}$  and  $f$  the Coriolis parameter at latitude  $48^\circ \text{N}$ . In both years we find a weak net off-shelf wind-driven surface Ekman transport of  $0.1\text{--}0.2 \text{ m}^2 \text{ s}^{-1}$ , which would drive a weak compensating on-shelf return flow in the bottom layer.

##### (3) Pressure-gradient flow

A consistent feature of all of the CTD sections is a cross-shelf

horizontal density gradient (Fig. 6) set up by the salinity gradient (Fig. 4a), and modified by seasonal changes in the horizontal temperature structure. The pressure gradients associated with contrasts in density across the outer shelf are conducive to driving on-shelf transports in the bottom layer (Fig. 10). Outside of the bottom turbulent boundary layer the pressure gradient will be balanced by Coriolis, and there would be no net transport down the density gradient. However, this balance breaks down in the bottom boundary layer, allowing down-gradient transport. We assume a simple balance between the horizontal pressure gradient ( $\frac{1}{\rho_0} \frac{\partial P}{\partial y}$ ) and stress,  $\tau$ , to occur within a bottom turbulent boundary layer of thickness  $h_{BL}$ :

$$\frac{1}{\rho_0} \frac{\partial P}{\partial y} = \frac{1}{\rho_0} \frac{\partial \tau}{\partial z} \quad (2)$$

Taking the vertical gradient in stress ( $\frac{\partial \tau}{\partial z}$ ) to be approximated by the effect of bed friction,  $\tau_b = k_b \rho_0 v^2$  with  $k_b \sim 0.0025$  the bottom drag coefficient,  $\rho_0$  the average density and  $v$  the mean current speed in the bottom layer, distributed through the bottom boundary layer,

$$\frac{1}{\rho_0} \frac{\partial P}{\partial y} = \frac{1}{\rho_0} \frac{k_b \rho_0 v^2}{h_{BL}} \quad (3)$$

for the total transport in the bottom boundary layer,  $h_{BL}$ , we have:

$$v h_{BL} = \sqrt{\frac{h_{BL}^3}{k_b} \frac{1}{\rho_0} \frac{\partial P}{\partial y}} \quad (4)$$

For  $h_{BL}$  we take the height above the seabed within which most of the velocity shear was located. Based on the current meter data available from the mooring at CCS this was  $\sim 40$  m. Density was depth averaged from the surface to 80 m depth for each oceanographic survey every 25 km between 100 km and the central Celtic Sea mooring site. The depth averaged density was used to calculate the pressure gradient force at 80 m along the hydrographic transect. In both years, the typical mean near bed pressure gradient term,  $\frac{1}{\rho_0} \frac{\partial P}{\partial y}$ , across the central shelf (between 100 and 350 km) from April to August was about  $0.7\text{--}1.2 \times 10^{-7} \text{ m s}^{-2}$ . Using these values in equation (3) gives velocities between 2.9 and 3.8  $\text{km day}^{-1}$  ( $0.03\text{--}0.045 \text{ m s}^{-1}$ ), which are of the same order to the ones calculated following the salinity contours (Fig. 4b), and a transport  $1.3\text{--}1.8 \text{ m}^2 \text{ s}^{-1}$ . This should be viewed as an upper limit, as we would expect some of this flow to be diverted across the pressure gradient by Coriolis.

#### (4) Internal tide Stoke's drift

The Celtic Sea is influenced by internal tidal waves, generated at the shelf slope and propagating at least 170 km into the Celtic Sea (Inall et al., 2011). At CCS semi-diurnal isopycnal displacements characteristic of a propagating internal tide first appear in April, shortly after the onset of stratification, and persist until December when the water column becomes isothermal again (Wihsgott, 2018). Evidence of isotherm displacement can also be found at the Celtic Deep, over 300 km from the shelf edge (not shown). The bottom layer Stoke's drift volume transport,  $V_{St}$ , associated with a propagating internal tidal wave is estimated from

$$V_{St} = \frac{1}{2} k A_0^2 \text{coth}(k h_b) \quad (5)$$

with  $k$  ( $\text{m}^{-1}$ ) the wavenumber,  $A_0$  (m) the wave amplitude and  $h_b$  (m) the bottom layer thickness (Simpson and Sharples, 2012). The wave speed is estimated from

$$c = \sqrt{\frac{g \Delta \rho}{\rho_0} h_b} \quad (6)$$

where  $g = 9.81 \text{ m s}^{-2}$ , and  $\Delta \rho$  is the bottom-surface density difference ( $\sim 1 \text{ kg m}^{-3}$ ). Using typical values for the wavelength (35 km) and

amplitude (15 m) for the internal tidal wave on the shelf (Inall et al., 2011) Eq. (5) suggests a volume transport of about  $1 \text{ m}^2 \text{ s}^{-1}$ . This on-shore Lagrangian transport has to be balanced by an offshore flow. Where in the water column that balancing return flow occurs will affect the net effect that the Stoke's transport has on bottom layer scalar distributions. If the return flow occurs within the pycnocline (e.g. Henderson, 2016) then  $1 \text{ m}^2 \text{ s}^{-1}$  would represent a reasonable estimate for the onshore bottom layer transport. There is some suggestion in the salinity transects for both summer 2014 and 2015 (Fig. 3) that there is offshore transport within the pycnocline layer, which would be consistent with this mechanism.

#### (5) High salinity lenses

High salinity lenses of water have been identified moving onshore within the pycnocline of the Celtic Sea (Hopkins et al., 2012), driven by non-linear second-mode internal waves. Combined with diapycnal mixing between the base of the pycnocline and the bottom layer, these would provide a mechanism for evolving the cross-shelf salinity gradient by transporting salt onto the shelf during the summer. An estimate of the volume flux driven by these lenses can be made by considering the mean flows associated with their onshore propagation ( $0.02 \text{ m s}^{-1}$ ) and the typical lens thickness (30 m) (Hopkins et al., 2012). This yields a transport of  $0.6 \text{ m}^2 \text{ s}^{-1}$ , which will be an upper limit due to the likely temporal patchiness in the generation of the internal waves and lenses (Hopkins et al., 2012). Whilst there is some evidence in August 2014 of higher salinities within the pycnocline near the shelf edge (Fig. 3c), there are also examples throughout the summers of both 2014 and 2015 of lower salinities than either the upper or lower layers (Fig. 3).

The above estimates suggest that the bulk of the on-shelf bottom layer flow may be a result of wind-driven Ekman transports, near bed pressure gradients and/or internal tide Stoke's drift. It seems unlikely that horizontal dispersion is able to contribute significantly to the on-shelf transport observed during early summer, and while high salinity lenses could in principle contribute we cannot find persistent evidence of the required salinity signal in the summer of 2014 and 2015.

#### 4.3. Offshore transports during winter

There is an indication in the salinity transects and evidence from the near bed currents recorded by the ADCPs across the shelf that water moves off-shelf between November 2014 and March 2015. While we lack CTD transect data through this period, we can make an assessment of the net effects of winter on the system by considering the changes in the horizontal salinity structure. The November CTD transect took place as the shelf water was quickly becoming fully-mixed by a combination of convection due to surface cooling and wind-driven mixing, and we know from the CCS mooring data that the shelf was vertically homogeneous by about mid-December (Wihsgott et al., this issue). The depth-mean salinity structure in November 2014 should therefore be very similar to that about 3 weeks later in mid-December, and we can compare that with the pre-spring salinity in March 2015 (Fig. 11). The  $35.45 \text{ g kg}^{-1}$  isohaline moves across the shelf by about 180 km between November and March, implying a cross-shelf flow of about  $2 \text{ cm s}^{-1}$  and a transport over 110 m depth of  $2.2 \text{ m}^2 \text{ s}^{-1}$ . Cross-shelf displacements of the higher value isohalines are less,  $\sim 70 \text{ km}$  for  $35.6 \text{ g kg}^{-1}$ ,  $\sim 40 \text{ km}$  for  $35.7 \text{ g kg}^{-1}$ . With mean depths associated with these isohaline movements of about 160 m and 170 m, this suggests transports of  $1.4$  and  $0.9 \text{ m}^2 \text{ s}^{-1}$ . AT CCS ADCP evidence indicates an offshore flow with mean velocities above  $1 \text{ km day}^{-1}$  between mid-November and February 2015. Similarly, at CD an offshore flow occurred between mid-November and April 2015, with maximum velocities ( $> 3 \text{ km day}^{-1}$ ) in December. Without more information over the winter it is difficult to be confident of the mechanisms driving these isohaline movements, but we can indicate likely causes.

The simplest explanation of the overall reduction in shelf salinity

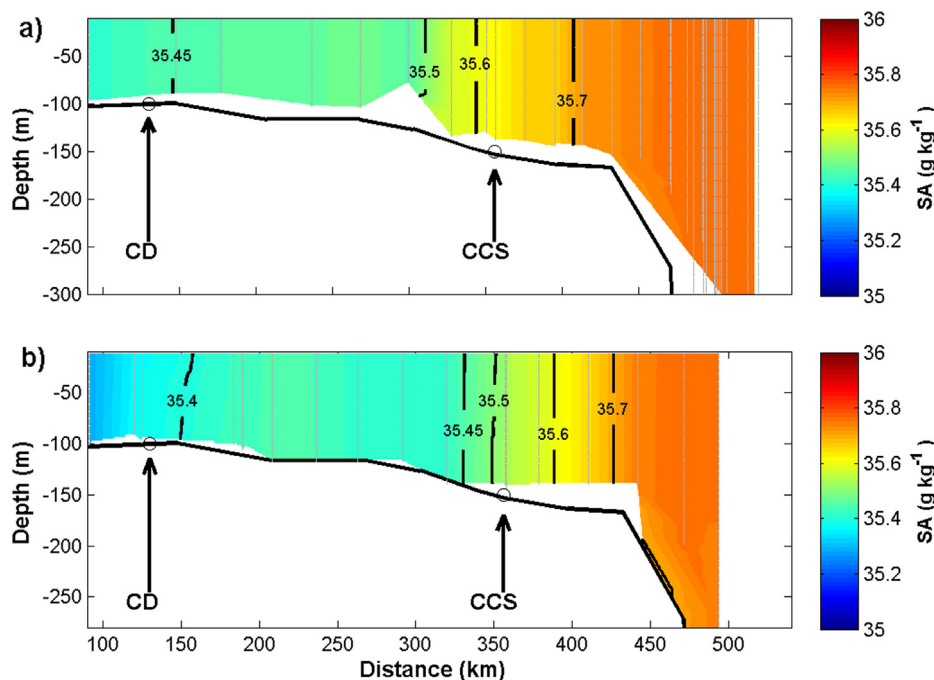


Fig. 11. (a) Depth-mean salinity in autumn (November 2014) and (b) Salinity distribution in late winter (March 2015).

between November and March is rainfall, with the strong winter mixing redistributing the freshwater vertically. Considering the mid-shelf between distances of about 150 and 300 km, the salinity decreased by about  $0.1 \text{ g kg}^{-1}$  over a mean depth of 100 m. Assuming no horizontal transport, and that the total mass of salt in the water column is conserved, then a precipitation of 31 cm would be sufficient to produce the observed salinity change. Between November and March the precipitation based on ERA-interim reanalysis was 16 cm at CCS and 18 cm at the Celtic Deep. Taking account of the ERA-interim precipitation over the ocean to be typically  $0.3 \text{ mm day}^{-1}$  higher than observations (Dee et al., 2011) reduces the precipitation by about 3 cm over the period November–March, suggesting that about 42–48% of the observed salinity change can be attributed to rainfall. At the outer shelf, between a distance of about 330 and 440 km, the observed salinity changes would need a rainfall of  $\sim 50 \text{ cm}$  and so about 26% of the salinity change is likely due to precipitation.

Based on the analysis of the effects of precipitation above, there remains a consistent off-shelf transport of about  $1 \text{ m}^2 \text{ s}^{-1}$  occurring over winter that needs to be explained. The along-shelf edge wind stress over the winter was seen to be consistently driving surface water off-shelf, with a mean Ekman transport of  $0.45 \text{ m}^2 \text{ s}^{-1}$ . Considering the cross-shelf horizontal salinity gradient this off-shelf flux would drive a decrease in surface salinity, with the compensating return flow increasing deeper water salinity. Towards the outer shelf the effect of depth-mean salinity can be estimated by taking a mean horizontal salinity gradient of  $1 \times 10^{-6} \text{ g kg}^{-1} \text{ m}^{-1}$  and assuming that the surface Ekman layer is about 30 m thick, with the return flow occurring in the lower 120 m. Over 3 months advection of the salinity gradient then yields a surface salinity decrease of  $0.12 \text{ g kg}^{-1}$ , and a bottom water salinity increase of  $0.03 \text{ g kg}^{-1}$ . Weighting these contributions by the layer thicknesses suggests almost zero change of the depth mean salinity. Taking into account the non-linearity of the horizontal salinity gradient, with the gradient tending to steepen at depth near the shelf edge, would lead to a slight salinity increase in the depth mean salinity of  $O(0.001 \text{ g kg}^{-1})$ . It is therefore unlikely that wind-driven Ekman transport can explain the overall reduction of shelf salinity and the implied off-shelf flux of  $1 \text{ m}^2 \text{ s}^{-1}$ . One possible candidate mechanism for this transport could be a flux through the bottom boundary layer driven by a cross-shelf pressure gradient. Assessing this is difficult

without further data between November and March: the problem largely depends on whether the excess cooling in the shallower water on the shelf, compared to the deeper outer shelf, can reverse the horizontal density gradient set up by the horizontal salinity gradient across the shelf.

#### 4.4. Implications for nitrate sources to the central Celtic Sea

The time series of nitrate at CCS allows us to make some inferences on the fate of nitrate throughout the year, and how the shelf is set up with nitrate ready for the spring bloom.

We have suggested, based on dilution and processing of riverine nitrogen, that the major riverine sources of nitrogen in the Bristol Channel could be responsible for about  $1 \text{ mmol m}^{-3}$  of the nitrate in the central Celtic Sea. There are two sources of error to these estimates. There is an uncertainty of about 15% in the empirical fit linking nitrate removal to transport timescale (Sharples et al., 2017), and there is uncertainty in the time it takes riverine water to be transported to the central Celtic Sea.

The on-shelf flow of bottom water during summer will also supply nitrate to the shelf. We can quantify this by using the time series of salinity from CTD at 80 m depth at CCS (Fig. 12) combined with a relationship between salinity and nitrate concentration across the shelf in March 2014, i.e. before the spring bloom and any biogeochemical modification of nitrate. There is a near linear increase in observed bottom water nitrate between April and November 2014, from  $8 \text{ mmol m}^{-3}$  to  $9.7 \text{ mmol m}^{-3}$  (Fig. 12b, dashed line). Of this  $1.7 \text{ mmol m}^{-3}$  increase,  $0.4 \text{ mmol m}^{-3}$  or 25% can be attributed to on-shelf transport in the bottom layer between March and August (Fig. 12b, solid line) using the nitrate-salinity relationship. The total depth at CCS was 145 m, which in summer we will assume was made up of a 40 m surface layer and a 105 m bottom layer. Within the bottom layer a  $0.4 \text{ mmol m}^{-3}$  nitrate increase, suggests a transport contribution to total water column nitrate at CCS of about  $40 \text{ mmol m}^{-2}$ . The on-shelf movement of isohalines at CCS slows between August and November (Fig. 4a) and only an additional  $0.05\text{--}0.1 \text{ mmol m}^{-3}$  nitrate is supplied by advection during this period. From late summer onwards the surface layer deepens, and by November has reduced the depth of the bottom layer to 85 m (Wihgott et al. this issue). Therefore

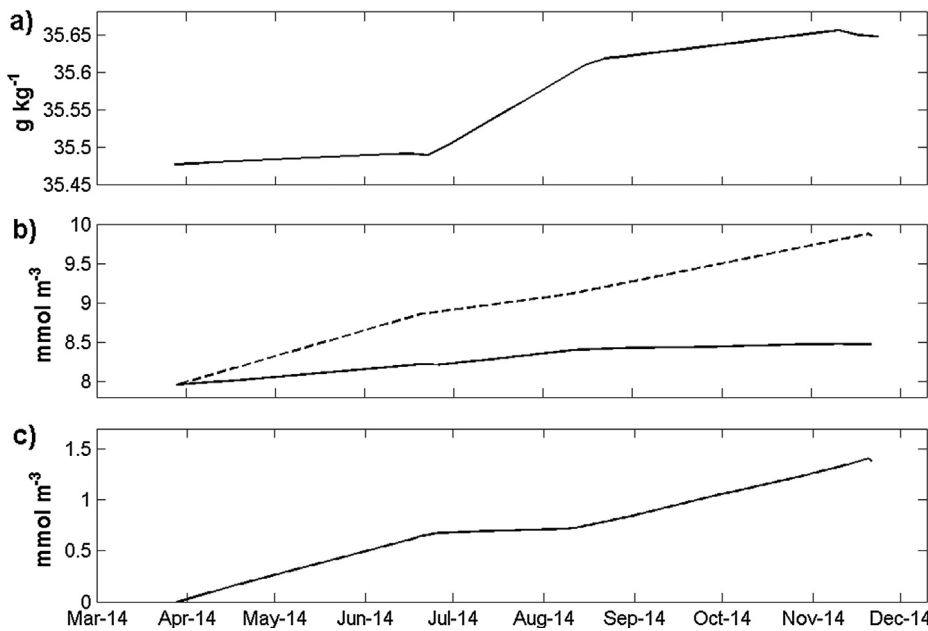


Fig. 12. (a) Bottom water salinity at CCS from CTD casts. (b) Observed nitrate concentration in CCS bottom water (dashed line) and nitrate concentration (black line) inferred from the movement of isohalines from the March 2014 nitrate-salinity relationship. (c) Difference between observed nitrate and the predicted supply from physical transport.

approximately  $7 \text{ mmol m}^{-2}$  of nitrate is transported to CCS in the bottom water during this later summer and early autumn period.

Pre-spring nitrate concentration at CCS in 2014 was  $8 \text{ mmol m}^{-3}$  in a water column of 145 m, so a total of  $1160 \text{ mmol m}^{-2}$  (Fig. 13a). At the end of August 2014 the 40 m deep surface layer was completely depleted in nitrate whereas the bottom 105 m saw an increase in nitrate concentration to  $9 \text{ mmol m}^{-3}$ , equating to a total water column DIN content of  $945 \text{ mmol m}^{-2}$  (Fig. 13b). The generation of organic material during the spring bloom, vertical fluxes of nitrate into the base of the thermocline sustaining a subsurface chlorophyll maximum during the summer months, on-shelf transport in the bottom layer and the regeneration of organic material all contribute to the  $215 \text{ mmol m}^{-2}$  total water column loss in nitrate during this period. Firstly, the spring bloom nitrate use is taken as the surface mixed layer thickness (40 m) multiplied by the initial pre-bloom nitrate concentration of  $8 \text{ mmol m}^{-3}$ , contributing a  $320 \text{ mmol m}^{-2}$  loss. The diapycnal nitrate

flux to the subsurface chlorophyll maximum, that we assume is all consumed, is estimated by using measurements of vertical eddy diffusivity made close to CCS by Williams et al. (2013). For the 4 months of May-August we assume a background  $1.5 \text{ mmol m}^{-2} \text{ d}^{-1}$  for 110 days, and storm driven fluxes of  $20 \text{ mmol m}^{-2} \text{ d}^{-1}$  for 10 days, giving a total loss of  $365 \text{ mmol m}^{-2}$ . Whereas nitrate is lost from the system to the spring bloom and SCM production, on-shelf transport in the bottom 105 m of the water column over the summer provides a  $40 \text{ mmol m}^{-2}$  increase to the total water column nitrate budget. Considering the change in nitrate concentration over the bottom 105 m between March and August ( $1 \text{ mmol m}^{-3}$  increase) and taking into account losses via diapycnal mixing ( $-365 \text{ mmol m}^{-2}$ ) and gains due to on-shelf advection ( $+40 \text{ mmol m}^{-2}$ ), there remains a  $430 \text{ mmol m}^{-2}$  excess in nitrate suggesting a significant amount of organic material has been regenerated in the bottom layer. Distributed over 105 m this equates to a concentration of  $4.1 \text{ mmol m}^{-3}$ , which would have originated from the

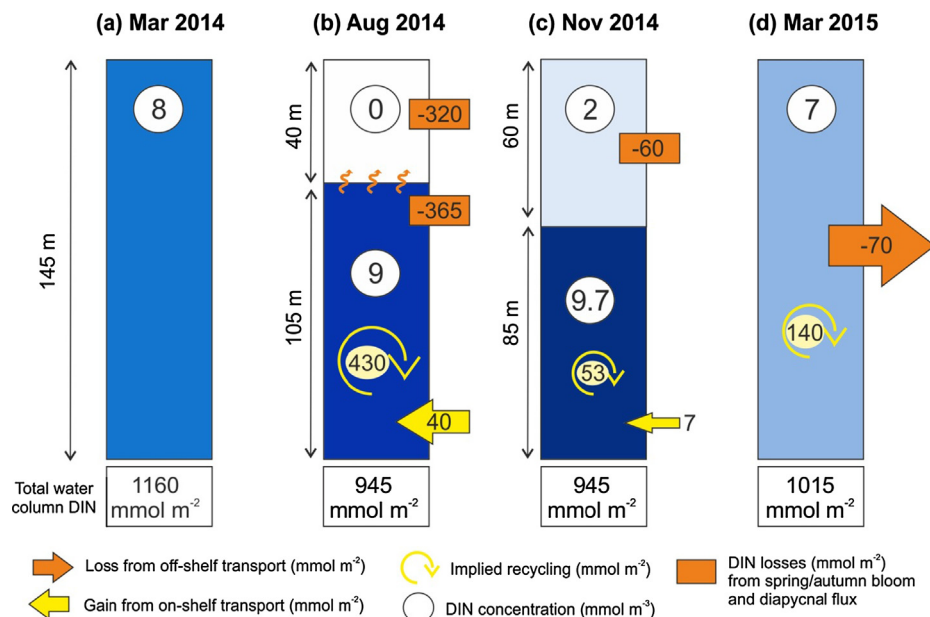
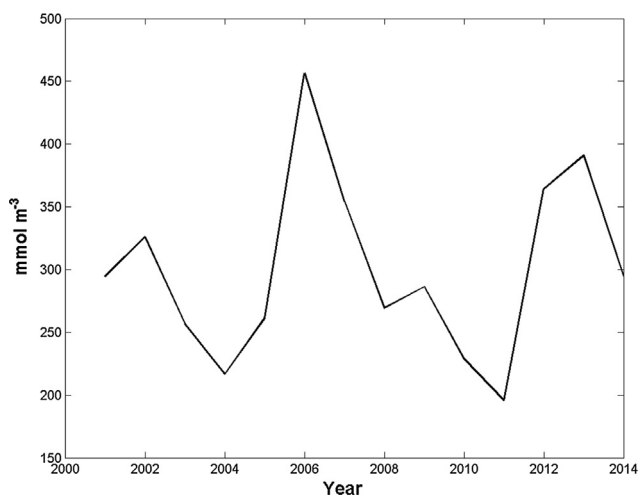


Fig. 13. Total water column dissolved inorganic nitrogen budget at CCS between March 2014 and March 2015 based on observed nitrate concentrations (in  $\text{mmol m}^{-3}$ ) and our estimates of bottom layer transport and nitrate uptake by phytoplankton. All losses and gains (in  $\text{mmol m}^{-2}$ ) are relative to the previous date.



**Fig. 14.** Averaged nitrate concentration input into the Bristol Channel during winter calculated from the river and nitrate time series. Each period covers the 1st of December to the 21st of March of the following year.

upper 40 m of the water column. Given the original pre-bloom concentration of  $8 \text{ mmol m}^{-3}$ , this implies that 51% of the nitrate taken up by the spring bloom had been recycled into the bottom layer by August. Note that this recycling estimate assumes that neither de-nitrification nor nitrate fluxes from sediments are significant.

The total water column nitrate in November was made up of a 60 m deep surface layer (nitrate concentration of  $2 \text{ mmol m}^{-3}$ ) plus a 85 m bottom layer (with  $9.7 \text{ mmol m}^{-3}$  nitrate), yielding  $945 \text{ mmol m}^{-2}$  (i.e. no change in total water column budget since August, Fig. 13c). Nitrate used by the autumn bloom is estimated by convectively mixing the August surface layer from 40 m to 60 m, entraining 20 m of water with  $9 \text{ mmol m}^{-3}$  nitrate concentration. Distributing this over the 60 m autumn mixed layer gives a concentration of  $3 \text{ mmol m}^{-3}$ . Knowing that in November only  $2 \text{ mmol m}^{-3}$  was observed in the surface layer,  $1 \text{ mmol m}^{-3}$ , or  $60 \text{ mmol m}^{-2}$ , is assumed to have been used by the autumn bloom by the time of the November survey. Between August and November there is an order of magnitude reduction in the advected bottom water supply of nitrate, estimated to be just  $7 \text{ mmol m}^{-2}$ . This is insufficient to explain the  $60 \text{ mmol m}^{-2}$  nitrate excess that accumulated between August and November ( $85 \text{ m} \times 0.7 \text{ mmol m}^{-3}$  concentration) and  $53 \text{ mmol m}^{-2}$  nitrate is therefore assumed to have been recycled. This represents 62% of the  $1 \text{ mmol m}^{-3}$  used during the autumn bloom.

By March 2015 the total water column nitrate had increased to  $1015 \text{ mmol m}^{-2}$  (Fig. 13d). Over winter the 145 m deep water column was fully mixed and nitrate concentrations pre-spring bloom in 2015 were  $7 \text{ mmol m}^{-3}$ . Off-shelf transport over the winter works to reduce the total water column nitrate at CCS. Taking into account the effect of winter rainfall, the reduction in nitrate is calculated by taking the depth-mean salinity and nitrate profiles in November 2014 and advecting them off-shelf to align with the depth-mean salinity in March 2015. This suggests that off-shelf advection reduces the total water column nitrate by  $70 \text{ mmol m}^{-2}$ . Knowing that there was a  $70 \text{ mmol m}^{-2}$  increase in total water column nitrate between November 2014 and March 2015,  $140 \text{ mmol m}^{-2}$  (approximately  $1 \text{ mmol m}^{-3}$  in 145 m water column) must have been either recycled and/or physically re-supplied.

The closeness of our nitrate budget estimate and the observed pre-bloom nitrate suggest that a combination of on-shelf advection of nitrate (25%) from the shelf edge during the summer and 50–62% recycling of organic nitrogen are sufficient to maintain the shelf nitrate pool. River supplies also make a contribution, potentially providing some of the  $140 \text{ mmol m}^{-2}$  required to close the budget in March 2015, but we again note the significant uncertainties in our understanding of

river nitrogen processing on the shelf and the transport time from the rivers to the mid and outer-shelf.

Finally, there is a  $\sim 1 \text{ mmol m}^{-3}$  difference in pre-spring nitrate concentrations across most of the shelf between 2014 and 2015. This implies significant inter-annual variability in the shelf nutrient pool, which likely arises from changes in the shelf edge and riverine boundaries as the main sources of nutrients to the shelf. An assessment of the winter freshwater nitrogen concentration (Fig. 14) indicates a range in the nitrogen concentration of  $200\text{--}450 \text{ mmol m}^{-3}$ , so a median of  $325 \text{ mmol m}^{-3}$  with a range of  $\pm 40\%$ . At CCS this would translate into a mid-range riverine nitrate contribution of  $0.8 \text{ mmol m}^{-3}$ , with a range of  $0.5\text{--}1.1 \text{ mmol m}^{-3}$ . Considering the shelf edge boundary, changing the depth of the winter mixed layer will alter the nitrate concentration boundary condition adjacent to the shelf. Typical winter mixed layer depths in the Northeast Atlantic range between 212 and 476 m (Hartman et al., 2014). Using the nitrate profile over the shelf slope in November 2014 and mixing it down to depths of 200 and 500 m changes the mixed layer nitrate concentration from 6.4 to  $8.9 \text{ mmol m}^{-3}$ . Our tentative suggestion therefore is that variability in both riverine nutrient supplies and the depth of the ocean winter mixed layer are significant in driving inter-annual variation of shelf nutrient pools, with the oceanic mixed layer depth being the most important.

## Acknowledgments

Sharples, Hopkins and Woodward were funded by the UK NERC-Defra Shelf Sea Biogeochemistry Programme (grant numbers NE/K002007/1, NE/K001701/1, NE/K002058/1). The Mexican National Council for Science and Technology (CONACyT) supported a scholarship to Eugenio Ruiz-Castillo. River nutrient data was kindly provided by Dr. Sonja van Leeuwen (Cefas, UK). The UK data was processed from raw data as provided from the Environment Agency, the Scottish Environment Protection Agency, the Rivers Agency (Northern Ireland) and the National River Flow Archive. Permission was granted from the Welsh Assembly to use data from the Welsh Rivers. All CTD, nutrient and mooring data is available from the British Oceanographic Data Centre. The authors thank Juliane Wihsgott for providing the CCS mooring data and Tom Hull for the Celtic Deep time series.

## References

- Behrenfeld, M.J., Boss, E., Siegel, D.A., Shea, D.M., 2005. Carbon-based ocean productivity and phytoplankton physiology from space. *Global Biogeochem. Cycl.* 19.
- Bowers, D.G., Roberts, E.M., White, M., Moate, B.D., 2013. Water masses, mixing, and the flow of dissolved organic carbon through the Irish Sea. *Cont. Shelf Res.* 58, 12–20.
- Brown, J., Carrillo, L., Fernand, L., Horsburgh, K.J., Hill, A.E., Young, E.F., Medler, K.J., 2003. Observations of the physical structure and seasonal jet-like circulation of the Celtic Sea and St. George's Channel of the Irish Sea. *Cont. Shelf Res.* 23, 533–561.
- Davis, C.E., Mahaffey, C., Wolff, G.A., Sharples, J., 2014. A storm in a shelf sea: Variation in phosphorus distribution and organic matter stoichiometry. *Geophys. Res. Lett.* 41. <https://doi.org/10.1002/2014GL061949>.
- Dee, D.P., Uppala, S.M., Simmons, A.J., Berrisford, P., Poli, P., Kobayashi, S., Andrae, U., Balmaseda, M.A., Balsamo, G., Bauer, P., Bechtold, P., Beljaars, A.C.M., van de Berg, L., Bidlot, J., Bormann, N., Delsol, C., Dragani, R., Fuentes, M., Geer, A.J., Haimberger, L., Healy, S.B., Hersbach, H., Hólm, E.V., Isaksen, I., Kållberg, P., Köhler, M., Matricardi, M., McNally, A.P., Monge-Sanz, B.M., Morcrette, J.-J., Park, B.-K., Peubey, C., de Rosnay, P., Tavolato, C., Thépaut, J.-N., Vitart, F., 2011. The ERA-Interim reanalysis: configuration and performance of the data assimilation system. *Q. J. R. Meteorol. Soc.* 137, 553–597. <https://doi.org/10.1002/qj.828>.
- García-Martín, E.E., Daniels, C.J., Davidson, K., Lozano, J., Mayers, K.M.J., McNeill, S., Mitchell, E., Poulton, A.J., Purdie, D.A., Tarran, G.A., Whyte, C., Robinson, C., 2017. Plankton community respiration and bacterial metabolism in a North Atlantic Shelf Sea during spring bloom development (April 2015). *Progr. Oceanogr.* <https://doi.org/10.1016/j.pocean.2017.11.002>. (this issue).
- Gowen, R.J., Stewart, B.M., 2005. The Irish Sea: nutrients status and phytoplankton. *J. Sea Res.* 54, 36–50.
- Hartman, S.E., Hartman, M.C., Hydes, D.J., Jiang, Z.-P., Snythe-Wright, D., Gonzalez, C., 2014. Seasonal and inter-annual variability in nutrient supply in relation to mixing in the Bay of Biscay. *Deep-Sea Res. II* 106, 68–75. <https://doi.org/10.1016/j.dsr2.2013.09.032>.
- Henderson, S.M., 2016. Upslope internal-wave Stokes drift, and compensating downslope Eulerian mean currents, observed above a lake bed. *J. Phys. Oceanogr.* 46, 1947–1961.

- Hickman et al., this issue. Seasonal variability in size-fractionated chlorophyll-a and primary production in the Celtic Sea. *Progr. Oceanogr.*
- Holligan, P.M., Williams, P.J., Purdie, D., Harris, R.P., 1984. Photosynthesis, respiration and nitrogen supply of plankton populations in stratified, frontal and tidally mixed shelf waters. *Mar. Ecol. Prog. Ser.* 17, 201–213.
- Holt, J., Wakelin, S., Huthnance, J., 2009. Down-welling circulation of the northwest European continental shelf: a driving mechanism for the continental shelf carbon pump. *Geophys. Res. Lett.* 36.
- Hopkins, J., Sharples, J., Huthnance, J.M., 2012. On-shelf transport of slope water lenses within the seasonal pycnocline. *Geophys. Res. Lett.* 39, L08604. <https://doi.org/10.1029/2012GL051388>.
- Horsburgh, K.J., Hill, A.E., Brown, J., Fernand, L., Garvine, R.W., Angelico, M.M.P., 2000. Seasonal evolution of the cold pool gyre in the western Irish Sea. *Prog. Oceanogr.* 46, 1–58.
- Horsburgh, K.J., Hill, A.E., Brown, J., 1998. A summer Jet in the St. George's Channel of the Irish Sea. *Estuar. Coast. Shelf Sci.* 47, 285–294.
- Houghton, R.W., Vaillancourt, R.D., Marra, J., Hebert, D., Hales, B., 2009. Cross-shelf circulation and phytoplankton distribution at the summertime New England shelf break front. *J. Mar. Syst.* 78, 411–425.
- Hull, T., Sivyver, D., Pearce, D., Greenwood, N., Needham, N., Read, C., Fitton, E., 2017. Shelf Sea Biogeochemistry – Celtic Deep 2 SmartBuoy. Centre for Environment Fisheries and Aquaculture Science, UK 10.14466/CefasDataHub.39.
- Huthnance, J.M., Coelho, H., Griffiths, C.R., Knight, P.J., Rees, A.P., Sinha, B., Vangriesheim, A., White, M., Chatwin, P.G., 2001. Physical structures, advection and mixing in the region of Goban spur. *Deep-Sea Res. II* 48, 2979–3021.
- Huthnance, J.M., Holt, J.T., Wakelin, S.L., 2009. Deep ocean exchange with west-European shelf seas. *Ocean Sci.* 5, 621–634.
- Hydes, D.J., Gowen, R.J., Holliday, N.P., Shammon, T.M., Mills, D., 2004. External and internal control of winter concentrations of nutrients (N, P and Si) in North West European Shelf Seas. *Estuar. Coast. Shelf Sci.* 59, 151–161.
- Inall, M., Aleynik, D., Boyd, T., Palmer, M., Sharples, J., 2011. Internal tide coherence and decay over a wide shelf sea. *Geophys. Res. Lett.* 38, L23607. <https://doi.org/10.1029/2011GL049943>.
- IOC, SCOR, IAPSO, 2010. The international thermodynamic equation of seawater –2010: calculations and use of thermodynamic properties. Intergovernmental Oceanographic Commission, Manuals and Guides No. 56, UNESCO, 196 pp.
- Jahnke, R.A., 2010. Global synthesis in “Carbon and Nutrient Fluxes in a Global Context, in Carbon and nutrient fluxes in continental margins”. *Glob. Synth.* 741.
- Jonas, P.J.C., millward, G.E., 2010. Metals and nutrients in the Severn Estuary and Bristol Channel: Contemporary inputs and distributions. *Mar. Pollut. Bull.* 61, 52–67.
- Linden, P.F., Simpson, J.E., 1988. Modulated mixing and frontogenesis in shallow seas and estuaries. *Cont. Shelf Res.* 8, 1107–1127.
- Liu, K.K., Atkinson, L., Quiñones, R.A., Talaue-McManus, L., 2010. Biogeochemistry of continental margins in a global context, in carbon and nutrient fluxes in continental margins. *Glob. Synth.* 741.
- Liu, K.-K., Tang, T.Y., Gong, G.C., Chen, L.Y., Shiah, F.K., 2000. Cross-shelf and along-shelf nutrients fluxes derived from flow fields and chemical hydrography observed in the southern East China Sea off northern Taiwan. *Cont. Shelf Res.* 20, 493–523.
- New, A.L., 1988. Internal tidal mixing in the Bay of Biscay. *Deep-Sea Res.* 35 (5), 691–709.
- New, A.L., Pingree, R.D., 1990. Evidence for internal mixing near the shelf break in the Bay of Biscay. *Deep-Sea Res.* 37 (12), 1783–1803.
- Pemberton, K., Rees, A.P., Miller, P.I., Raine, R., Joint, I., 2004. The influence of water body characteristics on phytoplankton diversity and production in the Celtic Sea. *Cont. Shelf Res.* 24 (17), 2011–2028.
- Pingree, R.D., 1980. Physical oceanography of the Celtic Sea and English Channel. In: Banner, F.T., Collins, M.B., Massie, K.S. (Eds.), *The North-West European Shelf Seas: the sea bed and the sea in motion II. Physical and Chemical Oceanography, and Physical Resources*. Elsevier Oceanography Series.
- Pingree, R.D., Le Cann, B., 1989. Celtic and Armorican slope and shelf residual currents. *Prog. Oceanogr.* 23, 303–338.
- Polton, J.A., 2015. Tidally induced mean flow over bathymetric features: a contemporary challenge for high-resolution wide-area models. *Geophys. Astrophys. Fluid Dyn.* 109, 207–215.
- Poulton, A.J., Davis, C.E., Daniels, C.J., Mayers, K.M.J., Harris, C., Tarran, G.A., Widdicombe, C.E., Woodward, E.M.S., this issue. Seasonal phosphorous and carbon dynamics in a temperate shelf sea (Celtic Sea). *Progr. Oceanogr.* 10.1016/j.pocean.2017.11.001.
- Roughan, M., Middleton, J.H., 2002. A comparison of observed upwelling mechanisms off the east coast of Australia. *Cont. Shelf Res.* 22, 2551–2572.
- Sanders, T.M., Garvine, R.W., 2001. Freshwater delivery to the continental shelf and subsequent mixing: an observational study. *J. Geophys. Res.* 106 (C11), 27087–27101.
- Seguro, I., Marca, A.D., Painting, S.J., Shutler, J.D., Sugget, D.J., Kaiser, J., this issue. High-resolution net and gross biological production during a Celtic Sea spring bloom. *Progr. Oceanogr.*
- Seitzinger, S., Harrison, J.A., Bohlke, J.K., Bouwman, A.F., Lowrance, R., Peterson, B., Tobias, C., Drecht, G.V., 2006. Denitrification across landscapes and waterscapes: a synthesis. *Ecol. Appl.* 16, 2064–2090.
- Sharples, J., Mayor, D., Poulton, A., Rees, A., Robinson, C., this issue. Preface: the UK Shelf Sea biogeochemistry research programme – seasonality in biogeochemical processes over a stratifying shelf sea. *Progr. Oceanogr.*
- Sharples, J., Middelburg, J., Fennel, K., Jickels, T.D., 2017. What proportion of riverine nutrients reaches the open ocean? *Global Biogeochem. Cycl.* <https://doi.org/10.1002/2016GB005483>.
- Simpson, J.H., 1976. A boundary front in the summer regime of the Celtic Sea. *Estuar. Coast. Mar. Sci.* 471–481.
- Simpson, J.H., 1981. The Shelf-sea fronts: implications of their existence and behaviour. *Philos. Trans. R. Soc. Lond. A* 302, 531–546.
- Simpson, J., Sharples, J., 2012. Introduction to the Physical and Biological Oceanography of Shelf Seas. Cambridge University Press pp. 424.
- Thompson, C.E.L., Sillburn, B., Williams, M.E., Hull, T., Sivyver, D., Amoudry, L.O., Widdicombe, S., Ingels, J., Carnovale, G., McNeill, C.L., Hale, R., Laguionie Marchais, C., Hicks, N., Smith, H.E.K., Klar, J.K., Hiddink, J.G., Kowalik, J., Kitidis, V., Reynolds, S., Woodward, E.M.S., Tait, K., Homoky, W.B., Kröger, S., Bolam, S., Godbold, J.A., Aldridge, J., Mayor, D.J., Benoist, N.M.A., Bett, B.J., Morris, K.J., Parker, E.R., Ruhl, H.A., Statham, P.J., Solan, M., 2017. An approach for the identification of exemplar sites for scaling up targeted field observations of benthic biogeochemistry in heterogeneous environments. *Biogeochemistry* 135, 1–34. <https://doi.org/10.1007/s10533-017-0366-1>.
- Thompson, C.E.L., Williams, M.E., Amoudry, L., Hull, T., Reynolds, S., Panton, A., Fones, G.R., 2018. *Cont. Shelf Res.* <https://doi.org/10.1016/j.csr.2017.12.005>. (in press).
- Thompson, R., Emery, W., 2014. *Data Analysis Methods in Physical Oceanography*, third ed. Elsevier, Amsterdam pp. 701.
- Uncles, R.J., 1984. Hydrodynamics of the Bristol Channel. *Mar. Pollut. Bull.* 15 (2), 47–53.
- Uncles, J., 2010. Physical properties and processes in the Bristol Channel and Severn Estuary. *Mar. Pollut. Bull.* 61, 5–20.
- Uncles, R.J., Radford, P.J., 1980. Seasonal and spring-neap tidal dependence of axial dispersion coefficients in the Severn – a wide, vertically mixed estuary. *J. Fluid Mech.* 98 (4), 703–726.
- Uncles, R.J., Stephens, J.A., 2007. SEA 8 Technical Report – Hydrography.
- Wihsgott, J.U., Sharples, J., Hopkins, J.E., Malcolm, E., Woodward, S., Greenwood, N., Hull, T., Sivyver, D.B., this issue. Investigating the autumn bloom's significance within the seasonal cycle of primary production in a temperate shelf sea. *Progr. Oceanogr.*
- Wihsgott, J., Hopkins, J., Sharples, J., Jones, E., Balfour, C.A., 2016. Long-term Mooring Observations of Full Depth Water Column Structure Spanning 17 Months, Collected in a Temperate Shelf Sea (Celtic Sea). British Oceanographic Data Centre – Natural Environment Research Council, UK doi: 10/bqwf.
- Wihsgott, J., Hopkins, J., Sharples, J., Balfour, C.A., Jones, E., 2018. Long-term, Full Depth Observations of Horizontal Velocities Spanning 17 Months, Collected in a Temperate Shelf Sea (Celtic Sea) on the NW European Shelf. British Oceanographic Data Centre – Natural Environment Research Council, UK doi:10/cjrh.
- Wihsgott, J., 2018. A Tale of Four Seasons: Investigating the seasonality of physical structure and its biogeochemical responses in a temperate continental shelf sea. Ph.D. Thesis. Department of Earth, Ocean and Ecological Sciences, University of Liverpool, UK.
- Williams, C., Sharples, J., Mahaffey, C., Rippeth, T., 2013. Wind-driven nutrient pulses to the subsurface chlorophyll maximum in seasonally stratified shelf seas. *Geophys. Res. Lett.* 40, 5467–5472. <https://doi.org/10.1002/2013GL058171>, 2013.
- Woodward, E.M.S., 2016. Discrete Inorganic Nutrient Samples Collected from the Celtic Sea During RRS Discovery Cruise DY026B in August 2014. British Oceanographic Data Centre – Natural Environment Research Council, UK doi: 10/bhpg.
- Young, E.F., Brown, J., Aldridge, J.N., Horsburgh, K.J., Fernand, L., 2004. Development and application of a three-dimensional baroclinic model to the study of the seasonal circulation in the Celtic Sea. *Cont. Shelf Res.* 24, 13–36.